MINISTRY OF SUPPLY

AERONAUTICAL RESEARCH COUNCIL
REPORTS AND MEMORANDA

The Calculation of Lift taking Account of the Boundary Layer

By

J. H. PRESTON, M.A., Ph.D., A.F.R.Ae.S.,
of the Cambridge University Aeronautics Laboratory

LONDON : HER MAJESTY'S STATIONERY OFFICE
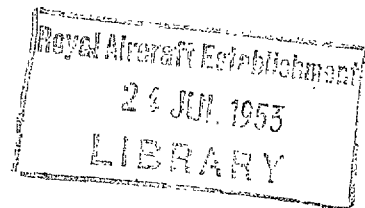
1953

PRICE 10s 6d NET

The Calculation of Lift taking Account of the Boundary Layer

By

J. H. Preston, M.A., Ph.D., A.F.R.Ae.S.,

of the Cambridge University Aeronautics Laboratory

Summary.—The purpose of this paper is to find a sound approach to the problem of the theoretical prediction of sectional characteristics taking account of the boundary layer.

Attention is mainly concentrated on the lift, since it is on the accuracy of this calculation that the accuracy of calculations for other characteristics such as pressure distribution and moments must depend. Calculations of the lift and of the velocity at the edge of the boundary layer near the trailing edge have been made for two dissimilar symmetrical aerofoils at an incidence of 6 deg, using boundary-layer data taken from experiment. The method of calculation satisfies the fundamental theorem that no net vorticity is discharged into the wake at the trailing edge and in contrast to the earlier calculations of R. & M. 1996, full account is now taken of the effect of the boundary layer on the velocity field outside the boundary layer, so that the empiricism of that report is avoided. The present calculations harmonise the two different methods of approach which have been used in the past, namely, the one in which the loss of lift below the Joukowski value was attributed entirely to the incidence and camber effects of the boundary layer, and the other in which the vorticity theorem was satisfied, but boundary-layer camber effects were ignored.

The main conclusions are as follows :—The calculated values of the lift and the velocity at the edge of the boundary layer at the trailing edge are in satisfactory agreement with experiment. Incidence and camber effects of the boundary layer account for a large proportion of the loss of lift, which is much greater for the Piercy 1240 aerofoil (trailing edge angle 22·15 deg) than for the cusped Joukowski aerofoil. Curvature effects may be important near the trailing edge. Prediction of the other characteristics such as pressure distribution and moments should be possible, but the work involved will be considerable. Given a satisfactory method of computing the details of the turbulent boundary layer up to the separation position, prediction of scale effects and Mach number effects on sectional characteristics below the stall should also be possible, using the methods of this paper in conjunction with an iterative process. More boundary-layer explorations should be undertaken in the neighbourhood of the trailing edge of large chord aerofoils with zero and finite trailing-edge angles.

---

1. *Introduction.*—The theoretical prediction of sectional characteristics, taking account of the boundary layer, is a necessary step towards the ultimate objective of predicting the behaviour of a wing of finite span. Potential flow calculations are useful in that they serve to provide orders of magnitude for some characteristics, which can also be regarded as limiting values when the Reynolds number is infinitely large. Thus the departure of a measured characteristic from its theoretical potential flow value is a measure of the influence of the boundary layer and some idea of the probable scale effects can be obtained. For instance, the measured lift slope for an aerofoil may be 90 per cent of the Kutta-Joukowski value in one case and only 70 per cent in another say, and we should therefore expect more serious scale effects for the second case. Similar arguments apply to the angle of no-lift, aerodynamic centre and C_{M0}. In the case of the drag, potential flow theory gives $C_D = 0$; whilst for hinge moments, the theoretical values represent

1

heavy under-balance, whereas in practice controls are designed to achieve close balance and hence scale effects may be serious. Again potential flow theory gives no guide to the value of C_L maximum to be expected. Whilst it is true that these characteristics can be measured, at Reynolds numbers approaching those of flight, in modern tunnels of low turbulence in the U.S.A., such equipment is very expensive and more economical use might be made of it through a better understanding of the influence of the boundary layer. In this country where such equipment has yet to be provided, theoretical prediction of boundary-layer effects is a necessity, if reliable results at flight Reynolds numbers are to be predicted from model data at Reynolds numbers from 10^6 to 10^7.

The success of the Squire and Young method (R. & M. 1838) in predicting the influence of Reynolds number, transition position and thickness, etc., on aerofoil drag and its value in assessing wind-tunnel and flight measurements naturally suggests the extension of boundary-layer calculations to other characteristics, particularly those relating to control surfaces. A first step to this end is the prediction of the circulation, since this governs the pressure distribution, on which the remaining characteristics depend. Attempts have been made in this country by Howarth[2] (1935), Piercy, Preston and Whitehead[3] (1938) and Preston (R. & M. 1996, 1943) to predict the circulation. All these attempts were based on a theorem first suggested by G. I. Taylor (R. & M. 989, 1924) which states that for steady motion the rates of discharge of positive and negative vorticity into the wake at the trailing edge are equal. A proof of this was given in R. & M. 1996 which was followed by a more rigorous and generalised analysis by Temple[6] (1943). The equality of rates of discharge of positive and negative vorticity was shown in R. & M. 1996 to imply continuity of pressure. In applying this condition, the pressure at a point in the wake must be the same, whether approached from above or below from points lying outside the wake— say along a line drawn normal to the streamlines, including the normal at the trailing edge. If the pressure rise through the wake is neglected, this leads to the approximate condition that the velocities at points on opposite sides of the wake on the same normal must be equal. The exact or the approximate condition enables the circulation to be fixed and the lift follows from $L = \rho U_0 \Gamma$. The circulation Γ for a real fluid must always be associated with paths which cut the streamlines in the wake at right-angles, otherwise, as G. I. Taylor showed (R. & M. 989), this relation no longer holds.

Howarth[2] applied this condition to the calculation of the lift of an elliptic cylinder, assuming a dead water region aft of the predicted separation points. The influence of the wake on the external potential flow was neglected. Piercy, Preston and Whitehead[3] also dealt with the same problem, but the influence of the wake was taken into account in an arbitrary fashion by the introduction of sources. Their computed lift curve was very similar to the experimental curve at moderate Reynolds numbers. In R. & M. 1996, the present author dealt with aerofoils at incidences sufficiently low to avoid turbulent separation, the condition of equal rates of discharge of positive and negative vorticity being applied at a normal to the streamlines at the trailing edge. It was assumed that the velocity field outside the boundary layer near the trailing edge could be computed with sufficient accuracy by neglecting the influence of the boundary layer and wake on this. Comparison with experiment, using measured values of the boundary-layer thickness, showed that only 30 per cent to 50 per cent of the difference between the experimental and Joukowski values of the lift could be accounted for in this way. The approximation that the velocities should be equal at points at the edge of the boundary layer on the normal to the streamlines at the trailing edge was fairly closely fulfilled in experiment, and errors arising from this source could in no way account for the discrepancies. Empirical corrections to the velocities at the edge of the boundary layer at the trailing edge were introduced, but although these gave values of the predicted lift which were in better agreement with experiment, the fact that they were not related to the boundary-layer configuration remained a strong objection to their use.

In order to assess the effect of the boundary layer on the velocity field outside the boundary layer, the author (R. & M. 2107) carried out calculations for a symmetrical Joukowski aerofoil at 0 deg incidence. The basis of this was the fact that the flow outside the boundary layer is closely given if the displacement thickness δ^* is added to the aerofoil to form a new shape, about which

the potential flow is computed. The maximum effect was found at the trailing edge, at the edge of the boundary layer; the effect on the velocity there amounting to an increase of about one per cent. Thus, when the aerofoil is at an incidence, it is clear that the mean displacement thickness of the two surfaces is not going to exert any important differential effect on the velocities on opposite sides of the trailing edge.

In searching for an explanation of the apparent failure of the vorticity condition to yield reasonable values for the computed lift the author was led to investigate the ' camber line ' effect of the displacement thickness δ^*. Now Stuper[8] (1933) in Germany, Pinkerton[9] (1936) and Nitzberg[10] (1944) in the U.S.A. have attempted to account for the loss of lift due to the boundary layer via a ' camber ' effect. They argued correctly that the effect of the boundary layer on the external flow could be represented by adding the displacement thickness δ^* to the two surfaces and thence there would be a camber equal to half the difference of δ^* for the two surfaces. Stuper[8] computed δ^*, using the momentum equation, for a Joukowski aerofoil and found that his computed lift was less than that given by the Joukowski hypothesis with no boundary layer, but no satisfactory experimental data were available for comparison. Pinkerton[9] took the measured lift and working back determined an arbitrary camber line, which, on a potential-flow basis using Joukowski's hypothesis, gave a lift in agreement with experiment. He then computed the pressure distribution for the new shape and obtained satisfactory agreement with experiment. Nitzberg[10] computed θ, the momentum thickness, from the momentum equation and assuming $\delta/\theta = 8 \cdot 4$, where δ is the boundary layer thickness, corresponding to an assumed $H \, \delta^*/\theta = 1 \cdot 4$ for the turbulent boundary layer, found δ for each surface. From the difference of δ for the two surfaces, he was able to construct an equivalent camber and compute the change in lift. He remarked that the correct course was to take δ^*, but in order to obtain computed lifts in reasonable agreement with experiment it was necessary to take δ. It is evident that his treatment of the momentum equation for turbulent flow is too approximate, since, except for very small pressure gradients, $H = 1 \cdot 4$ is incorrect and δ^* is seriously underestimated over the rear of the aerofoil on the upper surface. Thus the agreement of Nitzberg's calculated lift with experiment must be regarded as fortuitous.

In this paper the author will endeavour to show how the camber effect of δ^* and the requirement of equal rates of shedding of positive and negative vorticity into the wake at the trailing edge can be combined to yield calculated values of the lift, which are in satisfactory agreement with the experimental values. Moreover, the method rests on a sound theoretical basis. In order to remove a possible source of error, the calculations of lift have been made with values of δ^* taken from experiments on two symmetrical aerofoils 12 per cent thick, at 6 deg incidence (R. & M. 1998 and 2013). One aerofoil was a simple Joukowski shape with a cusped trailing edge, the other was a Piercy section with its maximum thickness at $0 \cdot 4C$ from the leading edge and trailing edge angle of $22 \cdot 15$ deg. The theory can be extended to include cambered aerofoil, with or without plain flaps and also to other characteristics and, provided δ^* can be computed with sufficient accuracy from the momentum equation, the prediction of scale effects and Mach effects becomes possible. Only the barest indication of the line of attack in these cases can be given in this report, the main purpose of which is to present the details of the lift calculation. It is on the soundness and accuracy of this calculation, that the calculation of the other characteristics, such as pitching moments and hinge moments, must depend. To this end, the theory has been kept as complete as possible and secondary effects arising from the boundary layer have been separated, where possible, from the major effects associated with aerofoil shape and their contributions to the final results are displayed.

2. Notation

α' = const.   denotes the equipotential lines in the irrotational flow about the aerofoil

β' = const.   denotes the streamlines in the irrotational flow about the aerofoil

s distance measured along the streamlines

n distance measured along the equipotential lines

3

h_0 velocity of potential flow about aerofoil with no boundary layer.

h velocity of potential flow in ξ-plane of aerofoil outside the boundary layer

$\zeta = \xi + i\eta$ complex co-ordinate on the plane of the aerofoil

$\zeta_1 = \xi_1 + i\eta_1$ complex co-ordinate in plane of plate, used in conjunction with aerofoil plus boundary layer camber

h_1 velocity of potential flow in the ζ_1-plane of the plate

$$m = \left| \frac{d\zeta_1}{d\zeta} \right|$$

$\zeta_2 = \xi_2 + i\eta_2$ complex co-ordinate in plane of plate, used in conjunction with basic aerofoil only

h_2 velocity of potential flow in the ζ_2-plane of the plate

$m_0 = |d\zeta_2/d\zeta|$

δ boundary-layer thickness, *i.e.*, value of n at edge of boundary layer

q velocity component in direction of lines $\beta' = $ const. for the real flow

w velocity component in direction of lines $\alpha' = $ const. for the real flow

U experimental value of q at the edge of the boundary layer

$$\psi^* \equiv \text{displacement flux} \simeq \int_0^\delta (U - q)\, dn$$

$$= \int_0^\delta (h_0 - q)\, dn \quad \text{more accurately}$$

$$\delta^* \equiv \text{displacement thickness} \simeq \int_0^\delta \left(1 - \frac{q}{U}\right) dn$$

More accurately it is defined by

$$\int_0^{\delta^*} h_0\, dn = \int_0^\delta (h_0 - q)\, dn$$

$$\theta \equiv \text{momentum thickness} = \int_0^\delta \left(\frac{q}{U} 1 - \frac{q}{U}\right) dn$$

$H = \delta^*/\theta$

u, l used as subscripts to denote ' upper ' and ' lower ' respectively.

δ_c^* centre-line change due difference of δ^* for the two surfaces

δ_s^* mean value of δ^* for the two surfaces

y negative camber of centre-line δ_c^*

α_1 incidence (negative) of centre-line δ_c^* relative to chord line

α_2 no-lift angle of camber line y

$\alpha_3 \equiv$ no-lift angle of centre-line $= \alpha_1 + \alpha_2$

α incidence of basic aerofoil

$$K_1 = \frac{\text{lift of aerofoil plus centre-line } \delta_c^*}{\text{lift of aerofoil for potential flow at incidence } \alpha}$$

x distance measured along chord of aerofoil

C chord of aerofoil

U_0 velocity at infinity

ρ density

Γ circulation

L lift

Γ_0 Joukowski circulation for aerofoil with no boundary layer

B point on edge of upper boundary layer on normal to streamlines through T

b point on edge of lower boundary layer on normal to streamlines through T

T trailing edge of basic aerofoil

T' fictitious trailing edge for aerofoil with boundary layer

ζ vorticity

P total pressure

$K_2 :$ $\dfrac{\text{circulation for equal shedding of positive and negative vorticity into wake}}{\text{circulation for flow to leave } T' \text{ smoothly}}$

$Z = X + iY = r \cdot e^{+i\theta}$ complex co-ordinate in plane of circle

$Z_1 = X_1 + iY_1 = r \cdot e^{i\theta_1}$ complex co-ordinate in plane of circle

     referred to axes rotated through $- \alpha_2$ relative to the X, Y-axes

a radius of circle

ε_τ trailing-edge value of ' ε ' in the Theodorsen-Garrick[12] theory

     $- \varepsilon_\tau =$ angle of no-lift

$- \beta$ angle of no-lift of basic aerofoil

W potential function

Δ_y (velocity)^2 increment factor at any point due to boundary-layer camber y.

Δ_s (velocity)^2 increment factor at any point due δ_s^*

C_L lift coefficient

$(C_L)_0$ lift coefficient of basic aerofoil with no boundary layer corresponding to the Joukowski value of the circulation

3. *Theory.*—3.1. *Boundary Condition at Edge of Boundary Layer and Definition of Displacement Thickness.*—It was shown in R. & M. 2107, that, in order to determine the potential flow outside the boundary layer, an inner boundary condition was needed at the edge of the boundary layer. Now from boundary-layer theory the direction of the streamlines entering the boundary layer relative to the aerofoil surface or relative to the streamlines with no boundary layer can be found. This gives the inner boundary condition for the potential flow external to the boundary layer. Neglecting curvature this can be satisfied by adding to the aerofoil the displacement thickness δ^* defined by

$$\delta^* = \int_0^\delta \left(1 - \frac{q}{U}\right) dn . \qquad\qquad\qquad\qquad\qquad (1)$$

The potential flow about this new shape is then computed and beyond the edge of the boundary layer it correctly takes account of the effect of the boundary layer, provided curvature is negligible. This idea of adding δ^* is an old one and previous to the publication of R. & M. 2107

' was derived from the fact that the streamlines outside the boundary layer are displaced outwards by an amount δ^* from the position they would have occupied if there had been no boundary layer. This displacement arises from the deficiency of flux (displacement flux) ψ^* defined by

$$\psi^* = U\delta^* = \int_0^\delta (U - q)\, dn\ . \qquad\qquad\qquad\qquad\qquad\qquad (2)$$

Now, as the trailing edge of the aerofoil is approached, the curvature of the streamlines becomes very large and hence the velocity of potential flow h_0 over a distance of the order of the boundary-layer thickness is no longer approximately constant and approximately equal to U, the velocity at the edge of the boundary layer. In fact, for an aerofoil with a finite trailing-edge angle, h_0 falls to zero at the trailing edge. The displacement flux is no longer given by equation (2), the correct expression being

$$\psi^* = \int_0^\delta (h_0 - q)\, dn\ , \qquad\qquad\qquad\qquad\qquad\qquad (3)$$

and the 'true' displacement thickness δ^* is defined by

$$\int_0^\delta h_0\ .\ dn = \frac{1}{U}\int_0^\delta (h_0 - q)\, dn\ . \qquad\qquad\qquad\qquad\qquad (4)$$

It is shown in Appendix 1, that if δ^*, as defined by equation (4), is added to the aerofoil, the streamlines enter the boundary layer at the correct angle very closely. The refinement in defining δ^* by (4) instead of (1) is only required in the immediate vicinity of the trailing edge.

3.2. *Camber Effect of Displacement Thickness.*—Let us take a symmetrical aerofoil for simplicity, at such an incidence that turbulent separation is absent and assume that the Reynolds number is high enough to avoid laminar separation. Then, owing to the more adverse pressure gradients over the upper surface, the displacement thickness δ^* and the boundary-layer thickness δ will be greater there than on the lower surface, particularly as the trailing edge is approached, where they merge to form the wake. This is illustrated diagrammatically in Fig. 1.
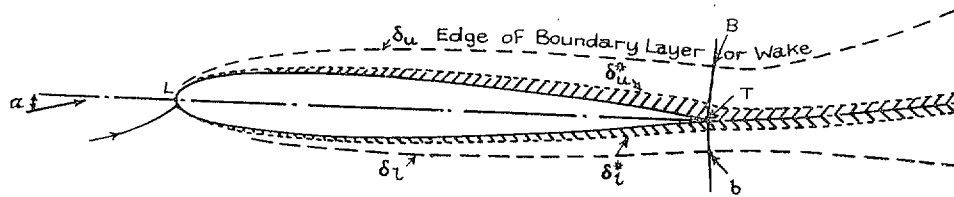
Fig. 1.

Now on the basis of the arguments in 3.1, we shall take correct account of the boundary layer, in so far as the external potential flow is concerned, if we add δ^* to the aerofoil and along either side of the dividing streamline in the wake, as shown diagramatically in Fig. 1. We can split this addition of δ^* up into two parts, a change of 'centre-line' δ_c^* given by

$$\delta_c^* = \tfrac{1}{2}(\delta_u^* - \delta_l^*)\ , \qquad\qquad\qquad\qquad\qquad\qquad (5)$$

plus an equal thickness contribution δ_s^* . to the two sides given by

$$\delta_s^* = \tfrac{1}{2}(\delta_u^* + \delta_l^*)\ . \qquad\qquad\qquad\qquad\qquad\qquad (6)$$

For the present, we shall be concerned with the antisymmetrical or centre-line contribution δ_c^*. Now, as will be shown in section 3.3, the camber change in the wake (if it exists) can be ignored, since the wake can exert no reaction on the surrounding fluid. The aerofoil can be disposed about the centre-line δ_c^* as shown in Fig. 2, with the 'effective' trailing edge T' at a distance

$$(\delta_c^*)_{\text{T.E.}} = \left(\frac{\delta_u^* - \delta_l^*}{2}\right)_{\text{T.E.}} \qquad\qquad\qquad\qquad\qquad (7)$$

above the actual trailing edge T.

6

FIG. 2.

As a first step, we determine the circulation for this cambered aerofoil using Joukowski's hypothesis that the flow shall leave the effective trailing edge T′ smoothly. This, from the nature of the centre-line, will be less than that of the basic aerofoil with no boundary layer, when the circulation is such that the flow leaves T smoothly. The circulation for the aerofoil with its new centre-line is computed as follows:
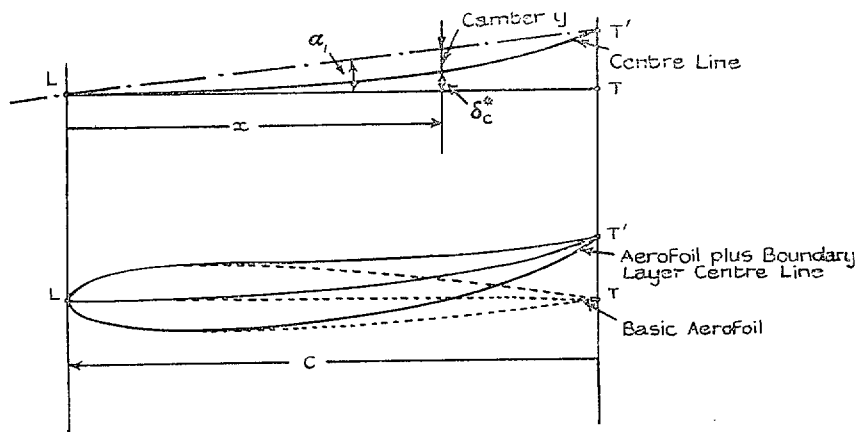
The centre-line δ^*_c may be considered as producing a reduction of incidence

$$\alpha_1 = \left(\frac{\delta^*_c}{C}\right)_{\text{T.E.}} = \left(\frac{\delta^*_u - \delta^*_l}{2C}\right)_{\text{T.E.}} \qquad \cdots \quad \cdots \quad \cdots \quad \cdots \quad \cdots \quad \cdots \quad (8)$$

and a *negative* camber-line, referred to LT′ as ' chord line ', given by :

$$y = \frac{x}{C}\left(\frac{\delta^*_u - \delta^*_l}{2}\right)_{\text{T.E.}} \frac{-\delta^*_u - \delta^*_l}{2} \qquad \cdots \quad \cdots \quad \cdots \quad \cdots \quad (9)$$

which produces a further reduction in lift.

α_1 and y are shown on Fig. 2.

Let us suppose the aerofoil with the centre-line δ^*_c turned to its no-lift incidence α_3, where

$$\alpha_3 = \alpha_1 + \alpha_2$$

in which α_1 represents the direct incidence effect of the centre-line given by equation (8) and α_2 is the no-lift angle of the camber y equation (9) and in practice is positive.

Define for any incidence ' α ' of basic aerofoil

$$K_1 = \frac{\text{lift of aerofoil with centre-line } \delta^*_c}{\text{lift of aerofoil without boundary layer}} \cdot \qquad \cdots \quad \cdots \quad \cdots \quad (10)$$

FIG. 3.

Then since the lift-slopes of the basic aerofoil without boundary layer and the basic aerofoil with the centre-line due to δ^*_c at a particular incidence α are the same (this centre-line is imagined to remain unchanged) we have from Fig. 3, for small α's

$$K_1 \simeq \frac{\alpha - \alpha_3}{\alpha} = 1 - \frac{\alpha_1 + \alpha_2}{\alpha} \qquad \cdots \quad \cdots \quad \cdots \quad (11)$$

at a chosen incidence α. By repeating this at different α's with the appropriate centre lines we can thus produce the lift-curve of the aerofoil with boundary layer on the Joukowski hypothesis that the flow leaves T′ smoothly.
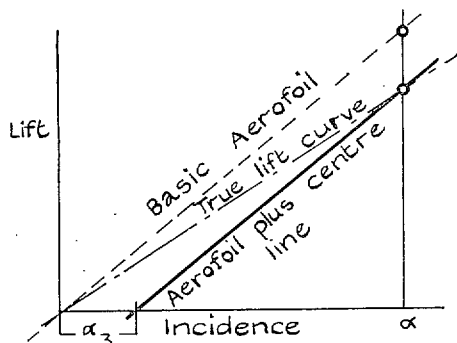
7

The no-lift angle α_2 due to the camber distribution y is given with sufficient accuracy by Glauert's ' thin ' aerofoil theory (*Elements of Aerofoil and Airscrew Theory*, p. 91)[11], where it is shown that

$$\alpha_2 = \frac{1}{\pi} \int_0^1 \frac{(y/C)\, d\left(\frac{x}{C}\right)}{(x/C)^{1/2}\left(1-\frac{x}{C}\right)^{3/2}} \qquad .. \qquad .. \qquad .. \qquad .. \qquad .. \qquad (12)$$

x being measured from the leading edge along the chord. The result is identical with that from the first approximation of the Theodorsen-Garrick[12] method, which is sufficiently accurate for aerofoils of normal thickness.

The above calculation of K_1 is identical in principle with the calculations made by Stüper[8], Pinkerton[9] and Nitzberg[10]. It shows the part which boundary-layer incidence and camber effects play in reducing the lift from the Kutta-Joukowski value for no boundary layer. Of more importance is the fact that it is a convenient step, which greatly aids the calculation of the final value of the circulation, which must satisfy the condition that the net flux of vorticity into the wake at the trailing edge is zero.

3.3. *The Flux of Vorticity across any Cross-Section of the Wake and the Condition for determining the Circulation.*—The calculation in the previous sub-section shows that applying Joukowski's hypothesis to the trailing edge T' of the centre-line obtained from the displacement thickness, the circulation so obtained is less than that for no boundary layer. This is not necessarily the circulation which satisfies the condition, suggested by G. I. Taylor (R. & M. 989, 1924), that as much positive as negative vorticity is discharged into the wake at the trailing edge.

This condition or theorem can be derived from a more general theorem given in Lamb's *Hydrodynamics*[19], which states that, ' The net flux of vorticity by convection and diffusion into any fixed closed circuit is equal to the rate of increase of circulation in that circuit.' If the motion is steady then the circulation is constant and the net flux of vorticity into the circuit is zero.
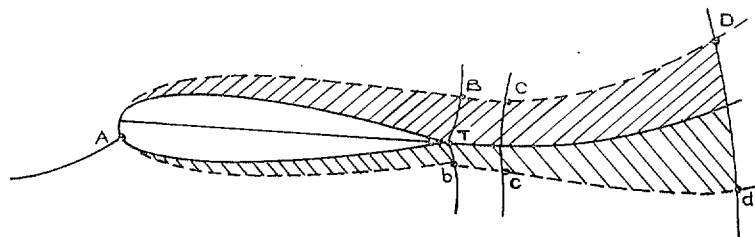
FIG. 4.

Turning to Fig. 4, in which an aerofoil and its boundary layer are indicated, and taking *any* circuit which encloses the aerofoil and its boundary layer and which cuts the wake in *any* manner, then for the part of the circuit outside the wake no vorticity enters and hence the net flux of vorticity out of the circuit via the wake must be zero, which is Taylor's condition. It therefore follows that, since all the vorticity is generated at the aerofoil surface and is diffused outwards and carried away by convection and diffusion *via* the wake, we must have

$$\oint \nu \left(\frac{\partial \zeta}{\partial n}\right)_{n=0} ds = 0, \qquad .. \qquad .. \qquad .. \qquad .. \qquad .. \qquad (13)$$

where ζ denotes the vorticity, S is the distance measured along the aerofoil surface and n is the distance measured normal to the surface. This result was derived by Cowley and Levy (R. & M. 715) in 1919 from the equations of motion on the physical basis of continuity of pressure. Thus continuity of pressure may be expected to be the exact condition for satisfying Taylor's condition of no net flux of vorticity into the wake and thus will fix the circulation. This aspect will be dealt with in detail later.

8

The fact that there is no net discharge of vorticity into the wake for steady motion was recognised intuitively by G. I. Taylor and led him to suggest that there is only one type of circuit for which the circulation Γ is constant and for which the relation

$$L = \rho . U_0 . \Gamma \qquad .. \qquad .. \qquad .. \qquad .. \qquad .. \qquad .. \qquad .. \qquad (14)$$

holds, *e.g.*, one which encloses the aerofoil and its boundary layer and which cuts the streamlines in the wake at right-angles. This was proved by the author in R. & M. 1996 and again by Temple[6] who generalised the results to include the effect of compressibility.

Again referring to Fig. 4 circuits ABTbA, ACcA and ADdA, which lie just outside the boundary layer and wake and which cut the streamlines in the wake at right angles, all have the same circulation. Consequently the circulation in circuits such as BCcbB, CDdcC and BDdbB is zero. It also follows from (13) and because the circulation is constant for all circuits enclosing the aerofoil and which cut the streamlines in the wake at right-angles, that there is no reaction from the wake on the external fluid in a direction normal to the stream at infinity.

It would seem that we can calculate the circulation Γ for any circuit of the type just described, since $L = \rho U_0 \Gamma$ for all such circuits. However, it is most convenient to choose a circuit whose path in the wake is formed by the normal passing through the trailing edge T. It is shown in R. & M. 1996 and also by Temple[6] that the rate at which vorticity ζ crosses BT, the upper normal, is

$$\int_T^B q\zeta \, dn = - \{P_B - (P_T)_u\}$$

and for bT, the lower normal

$$\int_T^b q\zeta \, dn = \{P_b - (P_T)_l\}$$

where P_B, P_b and P_T are the total pressures of the fluid at B, b and T. Now since B and b lie outside the boundary layer, by Bernoulli's theorem,

$$P_B = P_b .$$

At T

$$q = 0$$

and so

$$(P_T)_u = (p_T)_u$$
$$(P_T)_l = (p_T)_l$$

Therefore for

$$\int_T^B q\zeta \, dn = \int_T^b q\zeta \, dn$$

we must have

$$(p_T)_u = (p_T)_l . \qquad .. \qquad .. \qquad .. \qquad .. \qquad .. \qquad .. \qquad .. \qquad (15)$$

Thus p_T must be the same whether computed from above or below, which gives a condition for determining Γ.

It might be argued* that $(p_T)_u = (p_T)_l$ for all Γ, but this is not the case†. Let us ignore the pressure rise through the boundary layer, which in any case is quite small. For $(p_T)_u = (p_T)_l$ it follows from equation (15) that

$$U_B^2 = U_b^2 \qquad .. \qquad .. \qquad .. \qquad .. \qquad .. \qquad .. \qquad .. \qquad (16)$$

and there is only one value of Γ to give this. In general, the pressure rise through the two boundary layers is slightly different and for $(p_T)_u = (p_T)_l$

$$U_B^2 \simeq U_b^2 \qquad .. \qquad .. \qquad .. \qquad .. \qquad .. \qquad .. \qquad .. \qquad (17)$$

---

* *See* B. Thwaites. *A Note on the Determination of the Circulation about an Aerofoil.* A.R.C. 11,831. (Unpublished.)

† *See* J. H. Preston. *On the Determination of the Circulation about an Aerofoil.* A.R.C. 12,196. (Unpublished.)

If we take the value of $(U_B/U_b)^2 \simeq 1 \cdot 0$ from experiment or if we compute the pressure rise, we can find a value of Γ which will give the required $(U_B/U_b)^2$ such that the pressure is continuous in the wake.

Let us return to the aerofoil with its reflexed centre-line as found in section 3.2. Then, referring to Fig. 5, relative to the effective trailing edge T′, we have for the points B, b, which lie on the edges of the upper and lower boundary layers at the trailing edge,
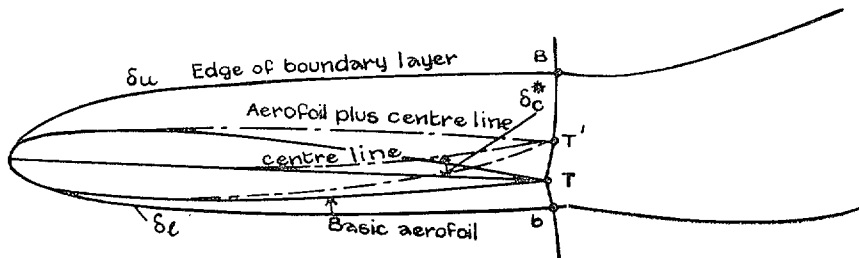
FIG. 5.

$$
\begin{aligned}
\text{BT}' &= (\delta_u - \delta_c{}^*)_{\text{T.E.}} = \left(\delta_u - \frac{\delta_u{}^* - \delta_l{}^*}{2} \right)_{\text{T.E.}} \\
\text{bT}' &= (\delta_l + \delta_c{}^*)_{\text{T.E.}} = \left(\delta_l - \frac{\delta_u{}^* - \delta_l{}^*}{2} \right)_{\text{T.E.}}
\end{aligned} \qquad \dots \quad \dots \quad \dots \quad (18)
$$

Let the circulation Γ, which satisfies the condition for equal rates of vorticity discharge at the trailing edge, be K_2 times that necessary for the flow to leave T′ smoothly. Then from equation (10)

$$ \Gamma = K_2 K_1 \times \Gamma_0 , \qquad \dots \quad \dots \quad \dots \quad \dots \quad \dots \quad (19) $$

where Γ_0 is the Joukowski value of the circulation for the aerofoil with no boundary layer. Before K_2 can be determined, we have to compute the velocities at B, b for a number of values of K_2. Then if equality of velocities at B, b is the determining condition, or if, from experiment or computation of pressure rise, a given velocity ratio is specified, we can interpolate to find K_2. *This calculation of the velocities at B, b, taking correct account of the boundary layer, is the crux of the problem of determining the circulation.*

3.4. *Velocity Calculations at the Edge of the Boundary Layer at the Trailing Edge.*—3.4.1. *Basic aerofoil and boundary layer camber effects.*—The method adopted follows that of R. & M. 1996 and is designed to utilise the series of charts prepared for that report. ·We take the basic aerofoil, plus its displacement thickness camber line y, corresponding to an incidence α of the basic aerofoil or an incidence $(\alpha - \alpha_1)$ relative to the line joining the leading edge L to the effective trailing edge T′.

FIG. 6.

10

Now any aerofoil can be conformably transformed into a circle by the Theodorsen-Garrick method[12]. In particular, the point corresponding to the trailing edge lies at an angle

$$\theta = \pi + \varepsilon_T , \qquad \qquad \qquad \qquad \qquad \qquad (20)$$

where ε_T corresponds to the angle of no-lift for the camber line, *i.e.*, α_2 given by equation (12). In our case, therefore, the position of T' in the plane of the circle is at

$$\theta = \pi - \alpha_2 . \qquad \qquad \qquad \qquad \qquad \qquad (20a)$$

If the axes in the Z-plane (circle) are rotated through an angle $-\alpha_2$ by the transformation

$$Z = Z_1 e^{-i\alpha_2} \qquad \qquad \qquad \qquad \qquad \qquad (21)$$

so that

$$\theta_1 = \theta + \alpha_2 \qquad \qquad \qquad \qquad \qquad \qquad (22)$$

then

$$\theta_1 = \pi$$

corresponds to the trailing edge T'. The transformation

$$\zeta_1 = Z_1 + \frac{a^2}{Z_1} \qquad \qquad \qquad \qquad \qquad \qquad (23)$$

transforms the circle radius a into a line of length $4a$ in the ζ_1-plane with T' at the point $\xi_1 = -2a$, $\eta_1 = 0$. The incidence of the stream at infinity relative to the new real axis in the circle plane and to the real axis in the ζ_1-plane is $(\alpha - \alpha_1 - \alpha_2)$. This is clearly shown in Fig. 6. The flow past the circle is given by

$$W = - U_0\left(Z' + \frac{a^2}{Z'}\right) - \frac{i\Gamma}{2\pi} \log_e \frac{Z'}{a} \qquad \qquad \qquad \qquad (24)$$

where

$$Z' = Z_1 e^{i(\alpha - \alpha_1 - \alpha_2)}$$

and Γ denotes the circulation.

The circulation, on the Joukowski hypothesis, which makes T' a stagnation point is

$$\Gamma_l = 4\pi a U_0 \sin (\alpha - \alpha_1 - \alpha_2) \qquad \qquad \qquad \qquad \qquad (25)$$

and

$$\Gamma = K_2 . \Gamma_1 = K_2 . 4\pi a U_0 \sin (\alpha - \alpha_1 - \alpha_2) . \qquad \qquad \qquad (26)$$

Note that

$$\Gamma_0 = 4\pi a U_0 \sin \alpha \qquad \qquad \qquad \qquad \qquad \qquad (27)$$

so that (25), (26), (27) are consistent with (19).

The velocity in the plane of the aerofoil h is given by

$$h^2 = \left| \frac{dW}{d\zeta} \right|^2 = \left| \frac{dW}{d\zeta_1} \right|^2 \times \left| \frac{d\zeta_1}{d\zeta} \right|^2 \qquad \qquad \qquad \qquad \qquad (28)$$

or

$$h^2 = h_1^2 m^2 , \qquad \qquad \qquad \qquad \qquad \qquad (29)$$

where, if

$$\zeta_1 = f(\zeta)$$

transforms the aerofoil plus the camber into the plate,

$$m^2 = \left| \frac{d\zeta_1}{d\zeta} \right|^2 \qquad \qquad \qquad \qquad \qquad \qquad (30)$$

and is independent of K_2 and α, depending only on the aerofoil shape and the camber line (including the boundary-layer camber),

11

and where

$$h_1{}^2 = \left| \frac{dW}{d\zeta_1} \right|^2 \qquad \text{..} \quad \text{..} \quad \text{..} \quad \text{..} \quad \text{..} \quad \text{..} \quad \text{..} \quad (31)$$

gives the velocity in the plane of the plate and is independent of aerofoil shape but is a function of $(\alpha - \alpha_1 - \alpha_2)$ and K_2.

It may be noted at this stage, that, up to the present, we have been dealing with a symmetrical aerofoil plus boundary-layer camber. The results are very easily generalised to include the case where the basic aerofoil has camber, whether produced by curving the centre line or by the deflection of a plain flap. Suppose the camber gives (in the usual notation) a potential flow no-lift angle of $- \beta$ on the Joukowski hypothesis, then we have to replace α_2 by $(\alpha_2 - \beta)$, wherever α_2 occurs in this section.

The advantage of referring to the ζ_1-plane, where the aerofoil plus the boundary-layer camber becomes a straight line, is that the normal to the potential flow streamlines at T$'$ is the straight line $\zeta_1 = - 2a$ at T$'$ in the ζ_1-plane. Any point distance n along the normal from T$'$ in the ζ_1-plane can be related to η_1 measured along the corresponding normal $\xi_1 = - 2a$ in the ζ_1-plane by use of equation (30) giving :—

$$m \, dn = d\eta_1 \qquad \text{..} \quad \text{..} \quad \text{..} \quad \text{..} \quad \text{..} \quad \text{..} \quad \text{..} \quad (32)$$

whence on integration

$$n = \int_0^{\eta_1} \frac{dn_1}{m} \qquad \text{..} \quad \text{..} \quad \text{..} \quad \text{..} \quad \text{..} \quad \text{..} \quad \text{..} \quad (33)$$

or

$$\frac{n}{C} = \frac{2a}{C} \int_0^{\bar\eta_1} \frac{d\bar\eta_1}{m} , \qquad \text{..} \quad \text{..} \quad \text{..} \quad \text{..} \quad \text{..} \quad \text{..} \quad \text{..} \quad (34)$$

where

$$\bar\eta_1 = \frac{\eta_1}{2a} . \qquad \text{..} \quad \text{..} \quad \text{..} \quad \text{..} \quad \text{..} \quad \text{..} \quad \text{..} \quad (35)$$

It should be noted that we assume that the normal to the real streamlines at the trailing edge is given sufficiently closely by the normal to the potential flow streamlines here.

Even when the aerofoil is symmetrical neither m nor n is an even function of $\bar\eta_1$, owing to the boundary-layer camber. It is desirable to separate the boundary-layer effect from that of the basic aerofoil by writing :—

$$m^2 = m_0{}^2 (1 + \Delta y)$$

where

$$m_0{}^2 = \left| \frac{d\zeta_1}{d\zeta} \right|^2 \qquad \text{..} \quad \text{..} \quad \text{..} \quad \text{..} \quad \text{..} \quad \text{..} \quad \text{..} \quad (36)$$

if

$$\zeta_1 = f_0(\zeta)$$

transforms the basic aerofoil in a plate in the ζ_1-plane and Δy represents the effect of the boundary-layer camber and is likely to be small. In this case Δy is to a close approximation an odd function of $\bar\eta_1$ and it arises from the fact, that, when the aerofoil plus camberline is in its no-lift position, there is a negative loading over the rear in practice, which, for points equi-distant from T$'$ along the normal, produces a (velocity)^2 increment $\Delta y \times m_0{}^2 \times U_0{}^2$, which is positive on the lower side and negative on the upper side. A method of computing Δy is given in Appendix II.

12

$m_0{}^2$ can be computed for a given shape of basic aerofoil as a function of $\bar\eta_1$ or n. When the aerofoil is symmetrical m_0 is an even function of $\bar\eta_1$ or n. If the aerofoil is derived from the circle by a simple conformal transformation, the calculation can be made directly at chosen values of $\bar\eta_1$ and n/C is computed from (34) where it is sufficient to write m_0 for m. Examples of such calculations are given in R. & M. 1996 and in Fig. 14 of this report. In the case of the arbitrary aerofoil, the velocity on the surface at zero lift must be computed by the Theodorsen-Garrick[12] method. The aerofoil surface is treated as a vortex sheet of strength equal to the surface velocity, and the velocity at chosen points not on the surface is found by integration, using the method suggested in Appendix I of R. & M. 2107 and also applied to the calculation of Δy in Appendix II.

Turning now to $h_1{}^2$, this has been plotted as $(h^2{}_p)/U_0{}^2$ against $\bar\eta_1$ in R. & M. 1996 for incidences of 3 deg, 6 deg and 9 deg, and for K ranging from $1 \cdot 0$ to $0 \cdot 5$. This is shown in Figs. 15, 16 and 17 of the present paper. These charts are still applicable to the present report if $(\alpha - \alpha_1 - \alpha_2) = 3$ deg, 6 deg, and 9 deg in turn, and with $K_2 = K$. Unfortunately our data refer to a specific α (in the present report this is 6 deg) and the values of $(\alpha - \alpha_1 - \alpha_2)$ will not be those used in the charts. However, if we imagine the boundary-layer centre-line for 6 deg and hence also $(\alpha_1 + \alpha_2)$ attached to other values of α, such that $(\alpha - \alpha_1 - \alpha_2) = 3$ deg, 6 deg, 9 deg in turn, and then find K_2 for these angles, we can obtain K_2 at the correct $(\alpha - \alpha_1 - \alpha_2)$ by interpolation.

3.4.2. *The effect of the $\delta_s{}^*$ component of δ^*.*—We have now to consider the effect on the velocity of the addition of $\delta_s{}^*$ (equation 6) to either side of the shape formed by the basic aerofoil and the camber v and also to either side of the wake centre-line. Typical variations of $\delta_s{}^*$ are shown in Fig. 13.
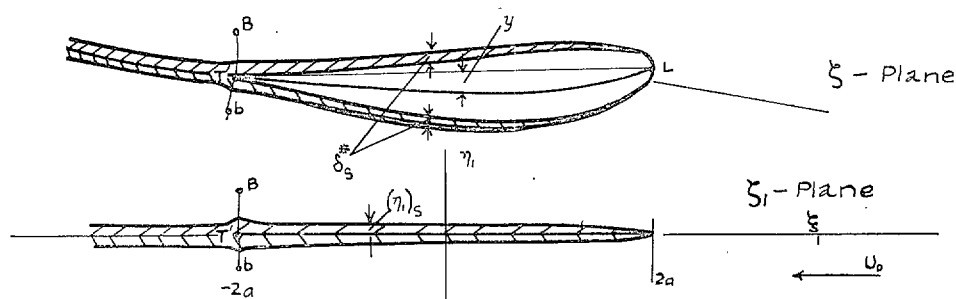

FIG. 7.

First imagine the cambered aerofoil turned to its no-lift angle $\alpha_{L=0} = \alpha_1 + \alpha_2$ and that $\delta_s{}^*$ remains unchanged. The transformation $\zeta_1 = f(\zeta)$ is then applied to convert the cambered aerofoil into a straight line. The boundary $(\eta_1)_s$ corresponding to the addition of $\delta_s{}^*$ can be found (*see* Appendix III). It is symmetrical about the ξ_1 axis and undergoes a comparatively rapid reduction at the trailing edge as in Fig. 7. The effect of this on the velocity field, which would otherwise be uniform $(= U_0)$ can be determined by the method of R. & M. 2107 or by the simplified version given in Appendix III. If $\frac{1}{2}\Delta_s U_0$ is the velocity increment parallel to the real axis at any point due to the source distribution which is equivalent to $(\eta_1)_s$, the resultant velocity is

$$h_1 \simeq U_0 + \tfrac{1}{2}\Delta_s U_0 \qquad \qquad \qquad \qquad \qquad \qquad (37)$$

and we write

$$\Delta_S = (h_1/U_0)^2 - 1 . \qquad \qquad \qquad \qquad \qquad \qquad (38)$$

We include this as part of the m^2 if the preceding section, so that it is now given by

$$m^2 = m_0{}^2 (1 + \Delta_y)(1 + \Delta_S) \qquad \qquad \qquad \qquad \qquad (39)$$

instead of by equation (36). Δ_S is an even function of $\bar\eta_1$, and in practice near the trailing edge, it represents a rise in velocity caused by the contraction of the streamlines of the boundary layer as they pass into the wake. The values of Δ_S at B and b are not equal since BT′ is generally greater than bT′.

13

3.4.3. *Final velocity.*—The final velocity h at any point outside the boundary layer along a normal at the trailing edge or other point on the surface in the plane of the aerofoil, is assumed to be given with sufficient accuracy by

$$\frac{h^2}{U_0^2} = m_0^2(1 + \Delta_y)(1 + \Delta_s) \cdot \frac{h_1^2}{U_0^2} \qquad \qquad \qquad \qquad \qquad (40)$$

where m_0 is a function of $\bar{\eta}_1$, determined by the basic aerofoil shape only, Δ_y is an odd function of η_1, depending on the camber y, Δ_S is an even function of η_1 depending on y_S, and h_1^2/U_0^2 is a function of $\bar{\eta}_1$, $(\alpha - \alpha_1 - \alpha_2)$ and K_2, which is given by charts, Figs. 15, 16 and 17 or from the formulae of Appendix I of R. & M. 1996.

The distance of the points B, b (marking the edge of the boundary layer) from T^1 the effective trailing edge (Fig. 5) are given by equation 18, so from the graphs connecting n/C with $\bar{\eta}_1$ — equation 34 and Fig. (14), we can determine $(\eta_1)_B$ and $(\bar{\eta}_1)_b$. Thus we can obtain $(h/U_0)_B^2$ and $(h/U_0)_b^2$ for various K_2 at $\{\alpha - (\alpha + \alpha_2)\} = 3$ deg, 6 deg and 9 deg. (Figs. 15, 16 and 17) and we put $(h_B/h_b)^2 = (U_B/U_b)^2$, where the value of $U_B^2/U_b^2 \approx 1\cdot 0$ is taken from experiment or assumed equal to $1\cdot 0$. Hence K_2 can be found for $\{\alpha - (\alpha + \alpha_2)\} = 3$ deg, 6 deg and 9 deg. The value of $(\alpha_1 + \alpha_2)$ corresponding to the chosen α of the basic aerofoil is obtained from the boundary-layer centre-line δ_c^* and so the value K_2 can be found by interpolation. When K_2 has been found it is a simple matter to obtain the velocities at the points B, b at the edge of the boundary layer at the trailing edge for comparison with those found by experiment.

3.5. *The Lift.*—The circulation Γ is found from

$$\Gamma = K_1 K_2 \Gamma_0 \qquad \qquad \qquad \qquad \qquad \qquad \qquad (19)$$

and since

$$\Gamma_0 = 4\pi a U_0 \sin \alpha \qquad \qquad \qquad \qquad \qquad \qquad (27)$$

$$L = \rho U_0 \Gamma \qquad \qquad \qquad \qquad \qquad \qquad \qquad (14)$$

$$C_L = (C_L)_0 K_1 K_2 , \qquad \qquad \qquad \qquad \qquad \qquad (41)$$

where

$$(C_L)_0 = 8\pi \frac{a}{C} \sin \alpha . \qquad \qquad \qquad \qquad \qquad \qquad (42)$$

4. *Experimental Data.*—In order to avoid errors in δ^* and δ, which may arise from attempting their prediction from turbulent boundary-layer theory and which might mask any shortcomings of the theory as set out in the preceding sections, it was decided to take δ^* and δ from experiments on two very different aerofoils. Both aerofoils were symmetrical, about 12 per cent thick and were derived from the circle by simple conformal transformations. One was a simple Joukowski aerofoil with a cusped trailing edge and maximum thickness at 25 per cent. The other was a Piercy aerofoil with its maximum thickness at 40 per cent and a finite trailing edge angle of $22\cdot 15$ deg. The experiments are described in R. & M. 1998 (Preston and Sweeting) and in R. & M. 2013 (Preston, Sweeting, and Cox). Measurements of δ^* and δ over the rear and in the wakes of the aerofoils at an incidence of 6 deg are available. The lift was also measured under approximately infinite stream conditions, so a direct comparison with the predicted values is possible. Figs. 9 to 12 show these data plotted as functions of x/C measured from the leading edge. Also shown are the centre line δ_c^*, camber y and thickness effects δ_s^* of the displacement thickness $\delta^*.\delta_c^*$ in the wake, it should be noted, is relative to the line of minimum velocity. The position of the line of minimum velocity relative to the chord line produced was not determined in the experiments quoted, owing to the unsuitability of the traverse gear. The discontinuity in the slope of δ_c^* at the trailing edge, therefore, may not exist and in any case the wake values are not required except to determine δ_c^* with better accuracy at the trailing edge. In addition the function $H = \delta^*/\theta$ is plotted and also δ^*/C for the two aerofoils at $\alpha = 0$ deg for comparison with the mean displacement thickness for 6 deg (Fig. 13). The lack of experimental points over the forepart of the aerofoil necessitated approximate calculations for this region, but it was apparent later that errors in this region are not important. A more serious difficulty

14

occurs at the trailing edge, where δ^* and δ change rapidly. It was assumed in interpreting the experimental data, that, up to the trailing edge, δ^* and δ increase steadily. This is supported by some recent American experiments described by Mendelsohn, N.A.C.A. T.N. 1304 (1947), and any theoretical predictions based on the momentum equation would almost certainly give this behaviour. The lower surface of the Joukowski aerofoil is an exception, since laminar separation occurs near this point. The true values of δ^* at the trailing edge were computed and are shown and the centre-lines and cambers based on these are also shown. The difference of shape between the two aerofoils clearly has a very marked effect on the development of δ^* and δ, on the magnitude of the boundary-layer centre-line, on the maximum camber and its position and on the thickness effect of the boundary layer. In fact, one can infer from these features that the Piercy 1240 aerofoil may be expected to have a smaller lift and a more positive hinge moment than the Joukowski aerofoil.

The ratios of the experimental lift to the theoretical (potential flow) lift, corrected for the effect of the bounday layers on the side walls of tunnel were:—

$$\left. \begin{array}{lll} \text{Simple Joukowski} & \dfrac{(C_L)_{\text{exptl.}}}{(C_L)_0} & = 0 \cdot 882 \\[4mm] \text{Piercy 1240 (wires)} & \dfrac{(C_L)_{\text{exptl.}}}{(C_L)_0} & = 0 \cdot 695 \end{array} \right\} \; \alpha = 6 \text{ deg.}$$

The experimental ratios of the (velocity)^2 on the two sides of the aerofoil at the edge of the boundary layer at the trailing edge were:—

$$\left. \begin{array}{lll} \text{Simple Joukowski} & \dfrac{U_B{}^2}{U_b{}^2} & = 1 \cdot 023 \\[4mm] \text{Piercy 1240 (wires)} & \dfrac{U_B{}^2}{U_b{}^2} & = 1 \cdot 000 \end{array} \right\} \; \alpha = 6 \text{ deg.}$$

The experimental (velocity)^2 at these points, corrected for the blockage caused by the mixing of the aerofoil boundary layer with the wind-tunnel wall boundary layer, were:—

$$\left(\frac{U_B}{U_0}\right)^2 = 0 \cdot 915$$

$$\text{Simple Joukowski} \qquad \left(\frac{U_b}{U_0}\right)^2 = 0 \cdot 893$$

$$\text{Piercy} \qquad \left(\frac{U_B}{U_0}\right)^2 = \left(\frac{U_b}{U_0}\right)^2 = 0 \cdot 860 .$$

The blockage correction was determined by comparing the experimental pressures in the wake with those for theory using the experimental circulation, where from R. & M. 2107 there are strong reasons for believing that at about $0 \cdot 1C$ behind the trailing edge the two distributions should run together if there were no blockage. This consideration gave corrections on the experimental (velocity)^2 in the tunnel of amounts $-0 \cdot 03$ for the simple Joukowski aerofoil and $-0 \cdot 04$ for the Piercy aerofoil.

5. *Calculations.*—Calculations of m_0 as a function of $\bar{\eta}_1$ were already available for the two aerofoils considered here and details of the methods employed are given in R. & M. 1996. Note that the present notation differs from that of R. & M. 1996.

In computing n/C as a function of $\bar{\eta}_1$ from equation (34) it was found that m^2 could be replaced by $m_0{}^2$ with sufficient accuracy for present calculations. Curves of $m_0{}^2$ and n/C as functions of $\bar{\eta}_1$ are given in Fig. 14.

$h_1{}^2/U_0{}^2$ (in the plane of the plate) as a function of $\bar{\eta}_1$ has been computed and plotted on charts in R. & M. 1996. The charts are reproduced here in Figs. 15, 16 and 17 for K_2 ranging from $1 \cdot 0$ to $0 \cdot 50$ and for $\alpha - \alpha_1 - \alpha_2 = 3$ deg, 6 deg, and 9 deg.

15

The 'true' values of δ^*/c at the trailing edge were next computed, as shown in Appendix I, equation 16 from the faired 'approximate' δ^*/c and from δ/c at the trailing edge, which are shown in Figs. 9 to 12. The centre-lines δ^*/c and camber lines y based on the approximate and true values of δ^*/c at the trailing edge were then obtained by equations 5 and 9. They are shown in Figs. 9 and 11. The lift calculations have been carried through for both sets of curves—the approximate being indicated by I and the true by II.

The angles α_1 (equation 8) and α_2 (equation 12) were next computed and from these K_1 (equation 11) was found.

The values of BT' and bT' (equation 18) were next found and expressed as n/c, whence by use of Fig. 14b the corresponding values of $\bar{\eta}_1$ in the plane of the plate were found. This enables m_0^2 at B, b to be obtained from Fig. 14a and h_1^2/U_0^2 for a range of K_2 for each $\alpha - \alpha_1 - \alpha_2 = 3$ deg, 6 deg and 9 deg from Figs. 15, 16 and 17. Δ_y, at B, b_1 was found from y as already described in Appendix II and Δ_S was found from δ_s^*, as indicated in section 4, 4b, and Appendix III. From equation 40, the final velocities h^2/U_0^2 at B, b for $\alpha - \alpha_1 - \alpha_2 = 3, 6, 9$ deg can now be tabulated for a range of K_2. It is convenient to plot the ratio $h^2{}_B/h^2{}_b$ against K_2. The correct value of K_2 is that for which $h^2{}_B/h^2{}_b$ equals the experimental value $U^2{}_B/U^2{}_b$ (if available) or unity if pressure rise through the boundary layer is neglected. Thus we obtain K_2 for $\alpha - \alpha_1 - \alpha_2 = 3, 6$ and 9 deg. In the present report, $\alpha = 6$ deg and $\alpha_1 + \alpha_2$ has been found for centre-lines I and II, and hence we can interpolate to find the appropriate K_2 and so finally we obtain $K_1 K_2$ which is the ratio of the predicted lift to that with no boundary layer on the Joukowski hypothesis. When K_2 is found the velocities at B, b, $i.e.$, (h^2/U_0^2)B, (h^2/U_0^2)b, can be found.

6. *Results*.—The main results are set out below in tabular fashion.

TABLE 1

$R = 4 \cdot 2 \times 10^5$ Simple Joukowski Aerofoil (Smooth) $\alpha = 6$ deg $= 0 \cdot 10472$ radn

Remarks	Quantity	Results	
		Based on δ^*. approx. I	Based on δ^* accurate II
Predicted for :—	α_1	0·00370 radn	0·00358 radn
	α_2	0·00398	0·00362
	$\alpha_1 + \alpha_2$	0·00768	0·00720
	K_1	0·927	0·931
	$(\Delta_y)_B$	−0·0069	−0·0064
	$(\Delta_y)_b$	0·0080	0·0074
	$(\Delta_S)_B$	0·0216	0·0163
	$(\Delta_S)_b$	0·0386	0·0175
$(U_B/U_b)^2 = 1 \cdot 0$	K_2	0·9595	0·9415
$(U_B/U_b)^2 = 1 \cdot 023,$	K_2	0·984	0·966
$(U_B/U_b)^2 = 1 \cdot 0,$	$(C_L/C_L)_0 = K_1 . K_2$	0·889	0·876
$(U_B/U_b)^2 = 1 \cdot 023.$	$(C_L/C_L)_0 = K_1 . K_2$	0·912	0·900
Experimental	$(C_L/C_L)_0$	0·882	
$(U_B/U_b)^2 = 1 \cdot 023$	$\begin{cases}(U_B/U_0)^2 \\ (U_b/U_0)^2\end{cases}$	0·914 0·893	0·903 0·884
Experimental	$\begin{cases}(U_B/U_0)^2 \\ (U_b/U_0)^2\end{cases}$	0·915 0·893	

16

TABLE 2

$R = 4\cdot2 \times 10^5$ Piercy 1240 Aerofoil (Turbulence Wires) $\alpha = 6$ deg $= 0\cdot10472$ radn

Remarks	Quantity	Results Based on δ^* approx I	Based on δ^* accurate II
Predicted for :—	α_1	0·00690 radn	0·00723 radn
	α_2	0·01388	0·01800
	$\alpha_1 + \alpha_2$	0·02078	0·02523
	K_1	0·802	0·7585
	$(\Delta_y)_B$	—0·020	—0·0292
	$(\Delta_y)_b$	0·020	0·0338
	$(\Delta_s)_B$	0·0712	0·0434
	$(\Delta_s)_b$	0·1012	0·0536
$(U_B/U_b)^2 = 1\cdot0$	K_2	0·9515	0·9565
$(U_B/U_b)^2 = 1\cdot0,$	$(C_L/C_L)_0 = K_1 \cdot K_2$	0·763	0·725
Experimental	$(C_L/C)_{L0}$	0·695	
		0·720 (based on Bryant's generalised curves.)	
Experimental	$(U_B/U_0)^2 = (U_b/U_0)^2$	0·883 | 0·855	
	$(U_B/U_0)^2 = (U_b/U_0)^2$	0·860	

7. *Discussion.*—7.1. *Present Results.*—From Tables 1 and 2 in the columns giving the results based on the accurate values of δ^*, it is seen that in the case of the simple Joukowski aerofoil the predicted $C_L/(C_L)_0 = 0\cdot900$ is greater than the experimental $C_L(C_L)_0 = 0\cdot882$ by about two per cent, while for the Piercy aerofoil the predicted $C_L/(C_L)_0 = 0\cdot725$ is greater than the experimental $C_L/(C_L)_0 = 0\cdot695$, by about four per cent. For this aerofoil at $R = 4\cdot2 \times 10^5$ using generalised curves given by Bryant[15] correlating experimental results on a trailing-edge angle basis, we should expect an experimental $C_L/(C_L)_0 = 0\cdot72$, so that the predicted value is in good agreement with this estimate. It is difficult to say whether the fact that the predicted values of $C_L/(C_L)_0$ are slightly greater than the measured values is of significance. There is the possibility of small errors in the experimental value of δ^*, δ and in the lift itself. The aerofoils used in the tests may not have accurately reproduced the theoretical shape in the region of the trailing edge. There is the difficulty that δ^* and δ at the trailing edge were not well defined experimentally and the calculated values of C_L depend on the interpretation of the measured values here. In addition, the factors Δ_y, Δ_s were not computed to a high accuracy because of the labour involved and the lack of precision in δ^* and δ near the trailing edge. In view of all these possible inaccuracies, it is considered that the predicted lifts are in satisfactory agreement with experimental results.

A further check on the method of calculation is furnished by the comparison of the velocities at the points B, b at the edge of the boundary layer at the trailing edge. Tables 1 and 2 show the predicted and measured (velocity)² to be in good agreement. This, at least, suggests that the theory, governing the deduction of δ^* accurate and the the calculation of Δ_s on which the velocity at B or b depends, is satisfactory.

The importance of the boundary-layer incidence and camber effect is shown by the values of α_1 and α_2 in relation to α and by the value of K_1 in Tables 1 and 2. The departure of the predicted lift from the Kutta-Joukowski value with no boundary layer is represented by $K_1 \times K_2$ and it is seen that K_1 accounts for most of it. K_2 does not differ greatly for the two aerofoils, but the values of K_1 do. From Figs. 9 and 11 showing δ_C^* and the camber it is seen that aerofoil shape

17

has a pronounced effect. The maximum boundary-layer camber is about $0 \cdot 12$ per cent for the Joukowski aerofoil and occurs at about $0 \cdot 6C$ from the leading edge, whereas for the Piercy aerofoil which has a trailing-edge angle of $22 \cdot 15$ deg, it is about $0 \cdot 34$ per cent occurring at $0 \cdot 8C$. This difference in camber explains in part why a cusped aerofoil with its position of maximum thickness well forward has a lift only some ten per cent less than the Kutta-Joukowski value for the aerofoil with no boundary layer, compared with the thirty per cent reduction suffered by an aerofoil with its maximum thickness further back and a trailing-edge angle of $22 \cdot 15$ deg. It also explains why plain controls on a cusped section tend to be heavily underbalanced, whereas those on a section with a large trailing-edge angle are over-balanced. However, further experiments, in which the course of the boundary layer is carefully explored near the trailing edge, are highly desirable, particularly as on cusped aerofoils the measured hinge-moment slopes apparently exceed the theoretical Joukowski values, though the lift slope is below the Joukowski value (*see* Bryant)[15] This, if true, implies a reversal of boundary-layer camber near the trailing edge and therefore very rapid changes in δ^* on the two surfaces in this region, which obviously increases the difficulties of calculation.

Turning now to the comparison between the calculations based on the approximate values of δ^* and those using the accurate values, we note on Figs. 9b and 11b that the centre-line component $(\delta_c{}^*)$ at the trailing edge is slightly less in the case of the Joukowski aerofoil and slightly greater in the case of the Piercy aerofoil when based on the accurate evaluation of δ^*. This difference is reflected in the camber y, Figs. 9c and 11c and in α_1, α_2, K_1 and Δ_y, Tables 1 and 2, and illustrates the relative sensitivity of these quantities to a small change of centre line $\delta_c{}^*$. As regards the thickness component $\delta_s{}^*$, Fig. 13a shows that the accurate value is considerably less than the approximate value at the trailing edge and it is presumed that a considerable rounding off of $\delta_s{}^*$ occurs in this neighbourhood, which is certainly more acceptable than the discontinuity of slope which occurs when the approximate values are taken. This rounding-off of $\delta_s{}^*$ greatly reduces $(\Delta_s)_B$, $(\Delta_s)_b$ and makes their values more nearly equal. It will be noted from Tables 1 and 2 that K_1 is reduced by increase of $\delta_c{}^*$ at the trailing edge, but because $(\Delta_y)_B$, $(\Delta_y)_b$ have their values numerically increased the effect of this is to increase K_2. On the other hand the evening up of the values of $(\Delta_Y)_B$ $(\Delta_y)_b$ tends to reduce K_2, so that no great change of K_2 takes place. Also, the predicted values of the (velocity)^2 at B, b have come out greater for the calculations using δ^* approx. The increments Δ_Y, Δ_S, though troublesome to calculate, cannot be neglected in general. For the Joukowski aerofoil, their neglect would not be serious and, in fact, would lead to a reduction in $(C_L/C_L)_0$ of about two per cent. In the case of the Piercy aerofoil their neglect would lead to a reduction in $(C_L/C_L)_0$ of about eleven per cent, thus bringing the calculated value well below the experimental value. The (velocity)^2 at the points B, b at the edge of the boundary layer would come out too low by a factor $\left\{ \dfrac{1 - (\Delta_S)_B + (\Delta_S)_b.}{2} \right\}$.

In the present calculations, we have fixed the circulation by making the calculated velocity ratio $(h_B/h_b)^2 = (U_B/U_b)^2$, the experimental velocity ratio. Neglect of curvature or, what amounts to the same thing, of pressure rise through the boundary layer gives $(h_B/h_b)^2 = 1 \cdot 00$ for no net discharge of vorticity into the wake. In the case of the Joukowski aerofoil the ratio $(U_B/U_b)^2 = 1 \cdot 023$ from experiment, but in the case of the Piercy $(U_B/U_b)^2 = 1 \cdot 00$. The pressure rise through either boundary layer at the trailing edge is certainly greater for the Piercy aerofoil than for the Joukowski aerofoil, but it so happens that the rise for the two sides is the same. This difference for the ratio $(U_B/U_b)^2$ is probably related to the totally different behaviour of δ^* for the lower surface near the trailing edge for the two aerofoils, Figs. 9a and 11a. There would be no difficulty in computing the pressure rise if the curvature of the streamlines and the velocity distribution along a normal to the trailing edge were known. However, in view of the closeness of the experimental ratio $(U_B/U_b)^2$ to unity it would be quicker to conduct experiments for aerofoils with different trailing edge angles and to relate the pressure rise to the boundary layer thickness and the trailing edge angle in an empirical manner. A change in $(U_B/U_b)^2$ from $1 \cdot 0$ to $1 \cdot 023$ is shown in Table 1 for the simple Joukowski aerofoil, where it is seen that $C_L/(C_L)_0$ is increased by about two per cent. A similar change in $(U_B/U_b)^2$ for the Piercy aerofoil would lead to a slightly

greater change of lift. It appears from experimental data that $(U_B/U_b)^2 > 1\cdot0$ for cusped aerofoils, but as the trailing-edge angle gets large $(U_B/U_b)^2 < 1\cdot0$ and from comparison with other aerofoils $(U_B/U_b)^2 = 0\cdot995$ might have been more acceptable for the Piercy aerofoil, thus giving a slightly smaller $C_L/(C_L)_0$ in Table 2.

7.2. *General Comments.*—The essence of the work described in this report is the calculation of the potential flow which effectively exists outside the boundary layer and wake. We seek a shape which, when added to the aerofoil, is such that the potential flow streamlines about the combined shape cross the line representing the edge of the boundary layer and wake at the angle which the streamlines cross in the real flow. Hence, outside the boundary layer and wake the fictitious and real flows are identical. Inside the boundary layer and wake we must appeal to boundary-layer theory or to experiment if we wish to obtain details of the flow. It may be noted that no attempt was made to fix the position of the wake, it being left free to set itself along the general direction of the flow about the aerofoil plus boundary-layer centre-line. Use was made of the idea of displacement flux in determining the additive shape which represents the effect of the boundary layer and wake, and the subsequent calculations were simplified by the introduction of symmetrical and antisymmetrical contributions of this shape to the aerofoil and by the use of thin aerofoil theory, involving vortex sheet theory and sources and sinks.

In R. & M. 2107, two additional methods were tried in the calculation of the effect of the boundary layer and wake on the flow past a symmetrical aerofoil at 0 deg incidence. In one, the vorticity at any section of the boundary layer was imagined to be concentrated at its centre of gravity in the form of a vortex sheet, and the contribution of this to the flow past the aerofoil with no boundary layer was determined for points lying outside the line representing the edge of the boundary layer and wake. In the other method, the actual distribution of the vorticity in the boundary layer and wake was used. Both these methods gave results in close agreement with the method employing a source-sink representation of the ' displacement flux '. The approximate condition for no net flux of vorticity into the wake, namely, that the velocities at the edge of the boundary layer on the normal to the streamlines at the trailing edge are equal, makes the accuracy of the lift calculation, in part, dependent on the accuracy of calculation of these velocities. These alternative methods could be employed in the case of the lifting aerofoil and would form a check on the velocity calculations at the edge of the boundary layer at the trailing edge, provided the strength of the vorticity can be obtained with sufficient accuracy in this region. The effect of trailing edge-strips described in R. & M. 1996 furnishes experimental evidence of the sensitivity of the lift to factors which affect the velocity field near the trailing edge.

The method of this report requires the definition of an actual edge to the boundary layer e.g., $n = \delta$. At first sight this may appear very objectionable for calculations of the kind which have been made in this report. However, for a turbulent boundary, in practice, the definition of an actual edge can be made in a consistent manner, as there is a relatively rapid approach of the total pressure to the free stream total pressure at the edge of the boundary layer. Moreover, errors in δ, in the main, only, affect the K_2 factor, which does not have a decisive influence on the final value of $(C_L/C_L)_0$, though small errors may be present in the final tabulated values which arise from errors in δ. Any objection to the use of δ can be overcome by applying the vorticity condition in the form that the pressure at the trailing edge T is the same whether approached from above or below along a normal to the streamlines, through T. The (velocity)^2, or, by Bernoulli's theorem, the pressure is computed at points which lie outside the boundary layer for various K_2. These can be transmitted to the trailing edge if the velocity distribution and the curvature of the streamlines are known. The correct value of K_2 is that which makes $(p_T)_l = (p_T)_u$. Such calculations, of course, would be considerably more laborious than those given here and require greater knowledge of the turbulent boundary than is at present available.

8. *Extension of the Calculations.*—8.1. *Pressure Distribution, Pitching Moment and Hinge Moments.*—Having determined the circulation, the next step is to compute the velocities or pressures at the edge of the boundary layer around the aerofoil employing the method already

used for computing the velocities at B, b, at the trailing edge. Such calculations would be rather tedious and laborious ; however, assuming they can be carried out, the pressures have then to be transmitted through the boundary layer to the aerofoil surface. This requires a knowledge of the velocity distribution through the boundary layer and the curvature of the streamlines. Except near the trailing edge this latter may be taken as constant through the boundary layer and equal to that of the aerofoil surface. In general, this curvature is likely to be small and so the pressure rise through the boundary will be very small and may be neglected, so that over most of the aerofoil, except near the trailing edge, the velocity calculations may be carried out at the surface itself—taking due account of boundary—layer camber and thickness effects. It may well prove when typical calculations have been made, that even in the trailing edge region itself, judicious extrapolation from the region where the curvature is small to the trailing edge where the pressure can be found, will suffice. Comparison of calculated and measured pressures at the surface will provide a severe test for the basic theory and the methods of calculation set out here.

The pitching moment and hinge moments can then be found by taking moments and integrating. The latter are the most likely to be seriously affected by errors in the surface pressures near the trailing edge.

8.2. *Scale Effects.*—The present calculations have been carried through with boundary-layer data taken from experiment and in section 8.1 it has been indicated how the velocities at the edge of the boundary layer and the surface pressures may be found. Given the velocity at the edge of the boundary layer and fixing the position of the transition points, and the Reynolds number, there is no difficulty in calculating the displacement thickness of the laminar boundary layer. The turbulent boundary layer can be calculated by semi-empirical methods such as that developed by Doenhoff and Tetervin[16] or the simpler version developed by Garner (R. & M. 2133). These are probably sufficiently accurate provided the separation position is not too closely approached and the curvature effects near the trailing edge (pressure rise through the boundary layer) are not large. Thus the displacement thickness on the usual definition can be found for either surface as far as the trailing edge. As regards the course of the displacement thickness in the wake there is at present no theory enabling this to be computed, but the momentum thickness θ can be found with sufficient accuracy and, therefore, in order to compute displacement thickness $H = \delta^*/\theta$ must be found. A limited appeal to experiment should suffice to determine H empirically, as H is known at the trailing edge and far down the wake it tends to $1 \cdot 0$. In any case, no great accuracy is required as this only affects the factor $\varDelta_S$ and this has no decisive effect on the circulation.

To start the calculation it is necessary to guess the circulation or take the Joukowski value. The potential flow velocity at the edge of the boundary may be taken as that at the surface—with a suitable guess at the trailing edge—the velocities here being taken as equal. The boundary-layer displacement thickness can, therefore, be found for both surfaces and for the wake. The circulation for this boundary-layer configuration is found as described in this report and the velocity at the edge of the boundary layer is computed anew as indicated in section 8.1. From the second approximation to the velocity distribution a second approximation to the displacement thickness is found, and the corresponding circulation is found which should be sufficiently accurate. Further iterations can, of course, be carried out if found to be necessary.

This operation can be repeated for other transition positions and Reynolds numbers and so, for a given wing, it should be possible to predict the sectional characteristic for incidences below the stall.

Prediction of the stall requires further development of the turbulent boundary-layer theory, as turbulent separation is not thought to be given with sufficient precision by existing theories. Moreover, little or no information exists on the behaviour of the boundary layer downstream of a turbulent separation. It will be evidence that as stalling incidence is reached, the upper boundary layer and the wake will be very thick and exert a considerable effect on the velocity field. The relatively crude calculations of Refs. 2 and 3 show that prediction of the stall is by no means hopeless, but considerable experimental investigations of the boundary-layer flow in this regime of incidence must be undertaken before such calculations can have any practical value.

8.3. *Mach Effects.*—The basic theorem relating to the constancy of circulation Γ in circuits enclosing the aerofoil and its boundary layer and which cut the streamlines in the wake at right-angles, the result that the net flux of vorticity into the wake at the trailing edge is zero and the relation

$$L = \rho_0 U_0 \Gamma ,$$

where ρ_0, U_0 refer to the stream at infinity, have not involved the continuity relation and hence are true for compressible flow (*see* Temple[6]).

The velocity field is, of course, affected by compressibility and the boundary layer will also be affected. The laminar boundary layer can probably be calculated for compressible flow with sufficient accuracy. The tubulent boundary layer has not yet received much attention, but the calculation by Young and Winterbottom (R. & M. 2400) represents a start in this direction. In R. & M. 1996 the assumption was made that the boundary-layer configuration was not affected by Mach number. It was then deduced that the circulation as predicted, taking account of the boundary layer, would be affected by Mach number in exactly the same way as the Joukowski value for potential flow. This is still true for the calculations of the present report. As experiment, in many cases, confirms this up the critical Mach number, it is concluded that Mach effects on the boundary-layer thickness are small and hence relatively crude calculations of these effects might suffice.

It would, therefore, appear that calculation of Mach effects up to the shock stall should be possible if the necessary extensions to turbulent boundary-layer theory can be made and checked experimentally.

9. *Conclusions.*—The calculations made in this paper show that satisfactory agreement has been obtained between predicted and measured lifts and between predicted and measured velocities at the edge of the boundary layer at the trailing edge for two quite different aerofoils. The differences which exist may be ascribed in part to possible errors in the measured values and in part to the interpretation put on the experimental data which were used in the calculations, and also to the fact that these data did not warrant more accurate, but laborious calculations of the effects of the displacement thickness on the velocities at the edge of the boundary layer.

In contrast to the calculations of R. & M. 1996 and those of Nitzberg[10], the calculations made here are free from empiricism and they have a sound theoretical basis. In the former the effects of the boundary camber and incidence were neglected and in the latter no attempt was made to satisfy the condition that there is no net flux of vorticity into the wake at the trailing edge. In this paper the basic ideas behind these previous two methods of predicting lift have been harmonised and I believe, in the broad sense, the result gives the correct method of approach to the problem, though the detailed calculations may possibly be improved.

Successful application of the method is dependent on the accuracy with which the boundary-layer camber and incidence can be predicted and on the accuracy of the calculation of the velocities at the edge of the boundary layer at the trailing edge.

The importance of boundary-layer camber and incidence effects is well brought out in this paper and they account for most of the drop of lift from the Joukowski value. The present calculations have utilised boundary-layer data taken from experiment and there is an element of uncertainty about these in the region of the trailing edge, which is sufficient to warrant further experimental investigations on large models in this region. Such data should be used to check existing turbulent boundary-layer theory, since the accuracy of *ab initio* calculations of lift and other characteristics will depend on the accuracy with which the turbulent boundary-layer characteristics can be predicted, particularly near the trailing edge, where curvature effects are becoming important.

The methods given in the appendices of calculating the velocity at the edge of the boundary layer might possibly be reviewed, particularly those which deal with the effect of the boundary layer, as distinct from aerofoil effects. The camber and thickness contributions of the displacement thickness change rather rapidly in the region of the trailing edge and some inaccuracy is

21

probably incurred by the present methods. As regards the contribution to the velocity made by the aerofoil, the charts of Figs. 15, 16 and 17 should be extended to cover 1 deg intervals of $(\alpha - \alpha_1 - \alpha_2)$ in order to make interpolation easier.

Having found the circulation there should be no difficulty in computing the pressures at the surface, except near the trailing edge where further research is needed to see how this can be done quickly and with sufficient accuracy. The pitching moment and hinge moment can then be found.

It would thus appear that for incidences below the stall we should be able, on existing turbulent boundary-layer theory, to calculate approximately the effect of transition position and Reynolds number on all the major sectional characteristics of an aerofoil. The stall (above the first appearance of turbulent separation) will require further experimental investigation and extension of turbulent boundary-layer theory and possibly refinement of the calculations set out in this paper. In addition, if the necessary extensions to present turbulent boundary theory can be made, we should also be able to predict the effect of Mach number on these characteristics up to the critical Mach number. These calculations, of course, represent a lengthy undertaking even for one aerofoil, but they would amply repay the labour by increasing our knowledge of the part played by these variables on the behaviour of sectional characteristics, and possibly lead to shorter methods of prediction which would be more suitable for routine investigations.

REFERENCES

No.	Author	Title, etc.
1	H. B. Squire and A. D. Young ..	The Calculation of the Profile Drag of Aerofoils. R. & M. 1838. 1937.
2	L. Howarth	The Theoretical Determination of the Lift Coefficient of a Thin Elliptic Cylinder. *Proc. Roy. Soc.* A, 149, pp. 558–586. 1935.
3	N. A. V. Piercy, J. H. Preston and L. G. Whitehead	The Approximate Prediction of Skin Friction and Lift. *Phil. Mag.* XXVI, p. 791. 1938.
4	J. H. Preston	The Approximate Calculation of the Lift of Symmetrical Aerofoils taking account of the Boundary Layer, with Application to Control Problems. R. & M. 1996. 1943.
5	L. W. Bryant and D. H. Williams	An Investigation of the Flow of Air Around an Aerofoil of Infinite Span with an Appendix by G. I. Taylor. R. & M. 989. 1924. Also *Phil. Trans. Roy. Soc.* A, 225. 1925.
6	G. Temple	Vorticity Transport and Theory of the Wake. A.R.C. 7118. 1943. (Unpublished.)
7	J. H. Preston	The Effect of the Boundary Layer and Wake on the Flow Past a Symmetrical Aerofoil at Zero Incidence. R. & M. 2107. 1945.
8	J. Stüper	Auftriebsverminderung eines Flügels durch seinen Widerstand. *Z.F.M.* 24, pp. 439–441. 1933,
9	R. M. Pinkerton	Calculated and Measured Pressure Distributions over the Midspan Section of NACA 4412 Aerofoil. N.A.C.A. T.R. 563. 1936.
10	G. E. Nitzberg	The Theoretical Calculation of Airfoil Section Coefficients at Large Reynolds Numbers. A.C.R. 4112. 1944.
11	H. Glauert	*Elements of Aerofoil and Airscrew Theory.* 2nd edit. Camb. Univ. Press.
12	T. Theodorsen and I. E. Garrick	General Potential Theory of Arbitrary Wing Sections. N.A.C.A. T.R. 352. 1933.
13	J. H. Preston and N. E. Sweeting	The Experimental Determination of the Boundary Layer and Wake Characteristics of a Simple Joukowski Aerofoil, with Particular Reference to the Trailing Edge Region. R. & M. 1998. 1934.
14	J. H. Preston, N. E. Sweeting and D. Cox	The Experimental Determination of the Boundary Layer and Wake Characteristics of a Piercy 12/40 Aerofoil, with Particular Reference to the Trailing Edge Region. R. & M. 2013. 1945.
15	L. W. Bryant	Two Dimensional Control Characteristics. Lift Due to Plain Flap. A.R.C. 9534. 1947. (To be published.)
16	A. E. von Doenhoff and N. Tetervin	Determination of General Relations for Behaviour of Turbulent Boundary Layers. N.A.C.A. T.R. 772. 1943.
17	H. C. Garner	The Development of Turbulent Boundary Layers. R. & M. 2133. 1944.
18	A. D. Young and N. E. Winterbottom	Note on the Effect of Compressibility on the Profile Drag of Aerofoils in the Absence of Shock Waves. R. & M. 2400. May, 1940.
19	H. Lamb	*Hydrodynamics.* 6th Edition. Paragraph 328a.
20	W. L. Cowley and H. Levy ..	An Analysis of the Steady Two-Dimensional Flow of an Incompressible Viscous Fluid. R. & M. 715.

APPENDIX I

Calculation of the True Displacement Thickness

1. *Conditions at the Edge of the Boundary Layer.*—Take a system of curvilinear co-ordinates α', β', defined by the equi-potentials and the streamlines of the potential flow about the basic aerofoil, with the Joukowski value of the circulation. α', and β' are identical with α and β as used in R. & M. 1996, the dashes being added to avoid confusion with α and β as used in the early part of this report to indicate angles.

Let h_0 be the velocity of potential flow for the basic aerofoil with no boundary layer, and ds, dn the lengths of the sides of the element $d\alpha'$, $d\beta'$ in the plane of the aerofoil.

Then

$$\left. \begin{array}{l} h_0 \cdot ds = d\alpha' \\ h_0 \cdot dn = d\beta' \end{array} \right\} \cdot \qquad \qquad \qquad \qquad \qquad \qquad \qquad (1)$$

Let q, w be the velocity components along the lines $\beta' = $ const. and $\alpha' = $ const. through any point for the real flow past the aerofoil. Then from Appendix I of R. & M. 1996, the equation of continuity is

$$\frac{\partial \bar{q}}{\partial \alpha'} + \frac{\partial \bar{w}}{\partial \beta'} = 0 , \qquad \qquad \qquad \qquad \qquad \qquad (2)$$

where

$$\left. \begin{array}{l} \bar{q} = q/h_0 \\ \bar{w} = w/h_0 \end{array} \right\} \cdot \qquad \qquad \qquad \qquad \qquad \qquad \qquad (3)$$

Let β_δ' be the value of β' corresponding to the edge of the boundary layer $n = \delta$. Then from equation (2) above

$$\bar{w}_\delta = - \int_0^{\beta_\delta'} \frac{\partial \bar{q}}{\partial \alpha'} \, d\beta' ,$$

$$= - \frac{d}{d\alpha'} \int_0^{\beta_\delta'} \bar{q} \, d\beta' + \bar{q}_\delta \frac{d\beta_\delta'}{d\alpha'}$$

$$= \frac{d}{d\alpha'} \int_0^{\beta_\delta'} (1 - \bar{q}) \, d\beta' - \frac{d\beta_\delta'}{d\alpha'} (1 - \bar{q}_\delta) . \qquad \qquad \qquad (4)$$

The angle which the real streamlines make with those of potential flow defined by $\beta' = $ const, at $\beta' = \beta_\delta$ is

$$\phi = \frac{\bar{w}_\delta}{\bar{q}_\delta} = \frac{1}{\bar{q}_\delta} \left\{ \frac{d}{d\alpha'} \int_0^{\beta_\delta'} (1 - \bar{q}) d\beta' - \frac{d\beta_\delta'}{d\alpha'} (1-\bar{q})_\delta \right\} . \qquad \qquad (5)$$

Now as a good approximation, when the boundary layer is thin and the circulation does not differ much from the Joukowski value

$$q_\delta = U \simeq (h_0)_\delta ,$$

i.e.,

$$\bar{q}_\delta \simeq 1 \cdot 0 .$$

24

Hence to this degree of approximation, equation (5) may be written

$$\phi \simeq \frac{d}{d\alpha'} \int_0^{\beta_\delta'} (1 - \bar{q}) \, d\beta'$$

$$= \frac{\delta}{d\alpha'} \int_0^\delta (h_0 - q) \, dn$$

$$= \frac{d}{d\alpha'} (\psi^*), \quad \quad \quad \quad \quad \quad \quad \quad \quad (6)$$

by definition

(*see* equation 3, section 4).

Now outside the boundary layer a potential flow exists, which differs slightly from that for the aerofoil with no boundary layer. The inner boundary condition for the flow is that the stream-lines enter the boundary layer at $n = \delta$ or $\beta' = \beta_\delta'$ making an angle ϕ (equation 6) with the line $\beta' = $ const., at this position. If this inner boundary condition can be satisfied, together with external boundary condition, which is fixed by the flow at infinity, then the flow outside the boundary layer is the correct one when the boundary layer is present.

2. *Method of Computing the Effect of the Boundary Layer.*—Transform the basic aerofoil into a straight line by $\zeta_2 = f_0(\zeta)$ and let

$$m_0 = \left| \frac{d\zeta_2}{d\zeta} \right|, \quad \quad \quad \quad \quad \quad \quad \quad (7)$$

where the ζ-plane is the plane of the aerofoil and the ζ_2-plane is that of the straight line. If h_2 is the velocity in ζ_2-plane and h_0 is the velocity in the ζ-plane, ignoring boundary-layer effects then

$$h_0 = h_2 \cdot m_0 .$$

If

$$\zeta_2 = \zeta_2 + i\eta_2 ,$$

the straight line into which the aerofoil is transformed forms part of the real axis

$$\eta_2 = 0 .$$

The angle ϕ (equation 6), at points on $\eta_2 = (\eta_2)_\delta$ in the ζ_2-plane corresponding to points on $\eta = \delta$ or $\beta' = \beta_\delta'$ in the ζ-plane, is unchanged by the transformation.

Now near the boundary

$$d\alpha' = h_0 (ds)_{n=0} = h_2 \cdot d\xi_2 ,$$

and so

$$\phi = \frac{d}{d\alpha'} (\psi^*) = \frac{1}{h_2} \frac{d}{d\zeta_2} (\psi^*) . \quad \quad \quad \quad \quad (8)$$

Now from R. & M. 2107, the appropriate source strength which deflects the streamlines of the required potential flow through this angle is

$$Q = \frac{d}{d\zeta_2} (\psi^*) \, d\xi_2 ; \quad \quad \quad \quad \quad \quad \quad (9)$$

these sources being distributed along the part of the real axis representing the aerofoil in the ζ_2-plane and along the dividing streamline, which springs from the trailing edge of the plate. Now the source strength is unaffected by the transformation and (9) may be written

$$Q = \frac{1}{h_2} \frac{d}{d\xi_2} (\psi^*) \, h_2 \cdot d\xi_2$$

$$= \frac{d}{d\alpha'} (\psi^*) \, d\alpha' . \quad \quad \quad \quad \quad \quad \quad (10)$$

25

Knowing ψ^*, we could, as in R. & M. 2107, proceed to compute the velocity increment due to this source distribution at required points on or outside the edge of the boundary layer. It is, however, more convenient to compute the equivalent change of aerofoil shape which will produce the same effect and to break up this change of shape into a change of centre-line plus equal contributions of thickness to the two sides of the aerofoil.

3. *Equivalent Change of Shape—True Displacement Thickness.*—The boundary formed by the closing streamline when the sources (equation 9) are introduced in the ζ_2-plane, is given (*see* R. & M. 2107) by

$$\eta_2^* \simeq \frac{\psi^*}{h_2}, \qquad .. \qquad .. \qquad .. \qquad .. \qquad .. \qquad .. \qquad .. \qquad (11)$$

since, for $0 < \eta_2 < (\eta_2)_\delta$, h_2, even near the trailing edge, is very closely constant, for all incidences, since curvature has been almost removed by the transformation. The boundary formed by the closing streamlines in the aerofoil or ζ-plane corresponding to $\eta_2 = \eta_2^*$ in the ζ_2-plane will be at $n = \delta^*$ say, where δ^* is now the true displacement thickness. We have

$$h_0 \, . \, dn = h_2 \, . \, d\eta_2 = d\alpha' \, . \qquad .. \qquad .. \qquad .. \qquad .. \qquad .. \qquad .. \qquad (12)$$

Hence

$$\int_0^{\delta^*} h_0 \, . \, dn = \int_0^{\eta_2^*} h_2 \, . d\eta_2 \simeq h_2 \, . \, \eta_2^* = \psi^* \, .. \qquad .. \qquad .. \qquad .. \qquad .. \qquad (13)$$

from equation (11).

But by definition (*see* section 4, equation 3)

$$\psi^* = \int_0^\delta (h_0 - q) \, dn \, .$$

Hence

$$\int_0^{\delta^*} h_0 \, . \, dn = \psi^* = \int_0^\delta (h_0 - q) \, dn \, . \qquad .. \qquad .. \qquad .. \qquad .. \qquad (14)$$

This may be regarded as the definition of the true displacement thickness δ^*.

Over most of the aerofoil, with the exception of the region in the immediate vicinity of the trailing edge, $h_0 \simeq U$, the experimental velocity at the edge of the boundary layer and equation (14) reduces to

$$U\delta^* = \psi^* = \int_0^{\delta^*} (U - q) \, dn$$

or

$$\delta^* = \int_0^\delta (1 - q/U) \, dn \qquad .. \qquad .. \qquad .. \qquad .. \qquad .. \qquad (15)$$

which is the approximate definition of δ^*

At the trailing edge, instead of using (14), we can proceed as follows if δ and δ^* approx. are known. Now (equation 11)

$$\eta_2^* = \frac{\psi^*}{h_2} = \frac{1}{h_2} \int_0^\delta (h_0 - q) \, dn \, ,$$

$$= \int_0^\delta \left(\frac{h_0}{h_2} - \frac{q}{h_2} \right) dn \, ,$$

$$= \int_0^\delta \left(\frac{h_0}{h_2} \right) dn + \frac{U}{h_2} \left[\int_0^\delta (1 - q/U) \, dn - \delta \right] .$$

Now

$$h_0 = h_2 \, . \, m_0 \, ,$$

hence

$$\eta_2^* = \int_0^\delta m_0 \, . \, dn \, \frac{U}{h_2} - (\delta - \delta^* \text{ approx.}) \, .$$

26

Now since

$$dη_2 = \frac{h_0}{h_2} dn = m_0 \cdot dn \,,$$

$$η_2{}^* = (η_2)_δ - \frac{U}{h_2}(δ - δ^* \text{ approx.}) \,.$$

Or

$$\barη_2{}^* = \frac{η_2{}^*}{2a} = (\barη_2)_δ - \frac{U}{h_2}\frac{C}{2a}(δ/C - δ^*/C \text{ approx.}) \qquad .. \qquad .. \qquad (16)$$

if the aerofoil of chord c transforms into a straight line of length $4a$. For h_2 we take the average value for $0 < \barη_2 < (\barη_2)_δ$.

Now at the trailing edge we have in Fig. 14b curves relating $\barη_2$ to n/c, hence we can find $(\barη_2)_δ$ corresponding to $n/c = δ/c$. Thus we can find $\barη_2{}^*$ and from the same figures we can read off the corresponding value of $δ^*$ true.

Note in Figs. 15, 16 and 17 that $(α_1 + α_2)$ in $α - (α_1 + α_2)$ is put equal to 0, since we are dealing with the basic aerofoil and the curve $K_2 = 1 \cdot 0$ is taken since h_0, $α'$, $β'$ refer to the Joukowski circulation for the basic aerofoil.

In the above calculation of the true displacement thickness, it will have been noted that the direction of the real flow streamlines entering the boundary layer was found relative to the direction of the potential flow streamlines about the aerofoil with no boundary layer and with the Joukowski value of the circulation. Now, if the actual circulation differs much from the Joukowski value, the flow outside the boundary layer would be better approximated by using the actual circulation—if known. In particular, the approximation made in the analysis that

$$q_δ = U \backsimeq (h_0)_δ$$

would be most closely fulfilled. On the other hand, this would lead to difficulties in evaluating $δ^*$ true in terms of $δ^*$ approx. at the trailing edge, since the potential flow would no longer leave the trailing edge smoothly and very rapid changes of the potential flow velocity would occur.

Now, except near the trailing edge, $δ^*$ true and $δ^*$ approx. should be the same very closely and the assumption

$$q_δ = U \backsimeq (h_0)_δ \,,$$

when (h_0) is now supposed constant over a distance comparable with $δ$, leads to this result, though as already mentioned, this assumption would be more closely fulfilled if the actual circulation or a good approximation to it were used. If we retain the Joukowski circulation, we will have to consider the accuracy of the calculation of $δ^*$ true at the trailing edge.

The results deduced by the method of calculation set out above show that the centre-line contribution $δ_c{}^*$ is very little different from the value based on the approximate definition. Now $δ_c{}^*$ via K_1 is responsible for the greater part of the loss of lift below the Joukowski value. Hence if we took the aerofoil with the centre-line, found in the approximate basis, and the Joukowski value of the circulation appropriate to the centre-line, e.g., $K_1 \cdot Γ_0$ the potential flow would leave T' smoothly, and since this circulation does not differ much from the actual circulation, the assumption that the actual velocities at the edge of the boundary layer are equal to the potential flow velocities at this position would now be more closely fulfilled. No essential change of procedure would be required in finding $δ^*$ true other than to note that the modulus of transformation from the aerofoil plus to boundary-layer centre-line to the plane of the plate would differ slightly from that for the aerofoil only, to the plate. For the cases dealt with this is small and would only affect the value of $δ^*$ true very slightly. Hence it is concluded that the calculations of $(δ^*$ true$)$ based on the use of the Joukowski circulation about the basic aerofoil are sufficiently accurate.

27

APPENDIX II

Calculation of Δ_y

Here we are ignoring the presence of δ^*_s and are concerned only with the camber y.

Δ_y is the factor which is related to the velocity increments arising from the boundary-layer camber y. If the transformation $\zeta_1 = f(\zeta)$ is applied so that the aerofoil plus camber line in the ζ-plane becomes a straight line in the ζ_1-plane, then from section 3.4, equations (29) and (36)

$$h^2 = m^2 h_1^2$$
$$= m_0^2(1 + \Delta_y)h_1^2 . \qquad \qquad \qquad \qquad \qquad (1)$$

If the aerofoil plus boundary-layer centre-line is placed at its no-lift incidence

$$\alpha = \alpha_1 + \alpha_2$$

then it follows from section 3.4 that

$$h_1^2 = U_0^2 \qquad \qquad \qquad \qquad \qquad \qquad \qquad (2)$$

and from (1) and (2)

$$h^2 = m_0^2(1 + \Delta_y)U_0^2 . \qquad \qquad \qquad \qquad \qquad (3)$$

Apply the transformation

$$\zeta_2 = f_0(\zeta)$$

to the aerofoil plus camber line in the ζ-plane, so that the basic aerofoil transforms into a straight line in the ζ_2-plane. Then,

$$\left. \begin{array}{c} m_0^2 = \left| \dfrac{d\zeta_2}{d\zeta} \right|^2 \\[2mm] \zeta_2 = f_0(\zeta) \end{array} \right\} . \qquad \qquad \qquad \qquad \qquad (4)$$

The aerofoil plus the boundary-layer camber line y will give very closely in the ζ-plane a camber line only, whose shape (provided the basic aerofoil is thin) is almost identical with the camber line y in the plane of the aerofoil. We assume that the camber lines are identical.

If h_2 is the velocity in the new ζ_2-plane, then, when the aerofoil plus camber line is at its no-lift position and since

$$h^2 = m_0^2 h_2^2 ,$$

it follows from (3) that

$$h_2^2 = U_0^2(1 + \Delta_y) . \qquad \qquad \qquad \qquad \qquad (5)$$

Hence if we can compute h_2^2 at desired points, we can obtain Δ_y from equation (5). Now the camber line in the ζ_2-plane is at its no-lift incidence and it is in effect a vortex sheet, we can compute its strength k by applying the thin aerofoil theory of Glauert[11] or by use of the Theodorsen-Garrick[12] method.
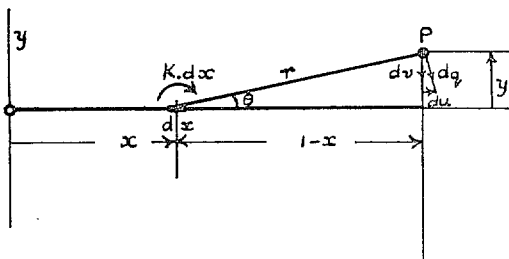
FIG. 8.

The velocity at the camber line is given by

$$h_2 = U_0 \pm k/2 .$$

The velocity at points not on the camber line can be obtained when the strength of the vortex sheet has been found. If the camber is small, then as in Glauert's thin aerofoil theory, we can take the vortex sheet along the chord line.

28

The circulation round an elementary vortex forming part of the vortex sheet is $k\,dx$ and with notation of the figure the velocity at a point P on the normal to the chord at the trailing edge is

$$dq = \frac{k\,dx}{2\pi r}$$

where

$$r^2 = (1-x)^2 + y^2$$
$\qquad \qquad \qquad \qquad \qquad \qquad$ (7)

It has components

$$du = dq \times \sin\theta = \frac{k\,dx \times y}{2\pi r^2}$$

$$dv = -dq \times \cos\theta = \frac{k\,dx \times (1-x)}{2\pi r^2}$$
$\qquad \qquad \qquad \qquad \qquad \qquad$ (8)

Whence by integration

$$u = \frac{y}{2\pi}\int_0^1 \frac{k\,dx}{(1-x)^2 + y^2}$$

$$v = \frac{1}{2\alpha}\int_0^1 \frac{k(1-x)\,dx}{(1-x)^2 + y^2}$$
$\qquad \qquad \qquad \qquad \qquad \qquad$ (9)

If u, v are small compared with the stream velocity U_0, then

$$h_2^2 = (U_0 + u)^2 + v^2 \simeq U_0^2(1 + 2u/U_0) \qquad \qquad \qquad (10)$$

and

$$\Delta y = \frac{2u}{U_0} = \frac{y}{\pi U_0}\int_0^1 \frac{k\,dx}{(1-x)^2 + y^2}. \qquad \qquad \qquad (11)$$

Now k is the strength of the vortex sheet at the no-lift incidence of the camber line. It can be considered as the sum of two distributions—one corresponding to the optimum incidence α_{opt} of the camber line in which k is finite everywhere, and the other giving a distribution proportional to $\alpha - \alpha_{opt}$ and varying as $\cot\phi/2$ where $\phi = \cos^{-1}(1 - 2x)$. This is the flat plate distribution and yields an infinite value for k at the leading edge $x = \theta = 0$. The contribution to Δy for this distribution can be obtained from the charts (Figs. 15, 16 and 17) by interpolation for the particular value of $\alpha - \alpha_{opt}$ and using the curves $K_2 = 1\cdot0$. Hence we must find α_{opt} for the camber line by thin aerofoil theory or otherwise.

The contribution to Δy from the α_{opt} distribution must be obtained by graphical or numerical integration of equation (11). It is unfortunate that the effective contribution to the integral equation (11) occurs over the last 20 per cent of the chord, which necessitates an accurate knowledge of k and hence of the camber in this region, and also the use of a large number of points. It is here where the weakness of the method lies, since the camber is determined from a faired curve through experimental points and hence no great accuracy can be expected for Δy.

It may be noted that when the loading at α_{opt} is of a simple form, e.g., constant or linear, then the integral in equation (11) can be evaluated analytically—the associated camber lines are easily obtained, and a rough estimate of Δy can be obtained by approximating to the experimental curve by one of these curves, or by a circular arc, for which Δy can also be found analytically, using conformal transformation.

APPENDIX III

Calculation of $\varDelta_s$

In section 3.4.2 the aerofoil plus camber y is transformed in to a straight line of length $4a.\delta_s{}^*$, which is symmetrically disposed about the aerofoil plus camber line, is carried with it to yield a thin symmetrical spear shaped boundary $(\eta_1)_s$ about the real axis in the ζ-plane of the straight line, when the aerofoil plus camber line is at its no-lift incidence. At the actual incidence for which the boundary layer data applies, the portion aft of the trailing edge is left free to follow the streamlines in this region. Ignoring $(\eta_1)_s$, then, for the no-lift incidence, the velocity $h_1 = U_0$ and so the problem resolves itself into finding $(\eta_1)_s$ from $\delta_s{}^*$ and then finding the effect of this on the velocity field at points lying beyond the boundary corresponding to the edge of the boundary layer, and in particular for those points at the edge of the boundary layer on a normal at the trailing edge.

We have

$$m = \left| \frac{d\zeta_1}{d\zeta} \right| \qquad \ldots \quad \ldots \quad \ldots \quad \ldots \quad \ldots \quad \ldots \quad \ldots \quad (1)$$

hence

$$m\,dn = d\eta_1 . \qquad \ldots \quad \ldots \quad \ldots \quad \ldots \quad \ldots \quad \ldots \quad \ldots \quad (2)$$

Now $\delta_s{}^*$ is small and m may be taken as constant over $0 < n < \delta$ except near the trailing edge.

Thus

$$(\eta_1)_s = m\delta_s{}^* . \qquad \ldots \quad \ldots \quad \ldots \quad \ldots \quad \ldots \quad \ldots \quad \ldots \quad (3)$$

Also

$$h = mU_0 \quad \text{at the no-lift position.} \qquad \ldots \quad \ldots \quad \ldots \quad \ldots \quad (4)$$

Thus

$$\left. \begin{aligned} (\eta_1)_s &= \frac{h}{U_0}\,\delta_s{}^* \\[2mm] &\simeq \frac{h_0}{U_0}\,\delta_s{}^* \end{aligned} \right\} \qquad . \quad \ldots \quad \ldots \quad \ldots \quad \ldots \quad \ldots \quad \ldots \quad (5)$$

Thus we require the potential velocity distribution over the basic aerofoil h_0. The trailing-edge value of $(\eta_1)_s$ is got from the curve showing n with $\bar\eta_1$, Fig. 14b, or it can be got by meaning the values of $\bar\eta_2{}^*\,c$ as found in Appendix I, equation (16).

As a satisfactory approximation we take $\xi_1/4a$ measured from the leading edge of the plate as being identical with ξ/c for the point in the plane of the aerofoil.

Having found the curve of $(\eta_1)_s$ as a function of $\xi_1/4a$, we now compute its effect on the velocity field at chosen points ξ_1, η_1 by the method of R. & M. 2107 by the introduction of sources.

The source strength, taking account of $(\eta_1)_s$ on both sides of the plate, is

$$dQ = 2U_0 \frac{d}{d\xi_1}(\eta_1)_s d\xi_1 \qquad \ldots \quad \ldots \quad \ldots \quad \ldots \quad \ldots \quad \ldots \quad (6)$$

and from R. & M. 2107 the velocity at points $\xi_1{}'$, $\eta_1{}'$, is given by

$$\frac{h_1}{U_0} = 1 + \frac{1}{\pi}\int_0^\infty \frac{d}{d\xi_1}(\eta_1)_s \cdot \frac{(\xi_1{}' - \xi_1{}')}{(\xi_1{}' - \xi_1)^2 + (\eta_1{}')^2}\,d\xi_1 \qquad \ldots \quad \ldots \quad (7)$$

and from (37) of the present report

$$\varDelta_s = \frac{2}{\pi}\int_0^\infty \frac{d}{d\xi_1}(\eta_1)_s \cdot \frac{(\xi_1{}' - \xi_1)}{(\xi_1{}' - \xi_1)^2 + (\eta_1{}')^2}\,d\xi_1 . \qquad \ldots \quad \ldots \quad (8)$$

For the purpose of computing the circulation $\varDelta_s$ is required at the points B, b at the trailing edge for which $\xi_1' = 4a$.

$\bar{\eta}_1'$ is obtained from Fig. 14b by reading off the value of $\bar{\eta}_1$ corresponding to $n/c = \mathrm{BT}'$ or bT' as required.

Hence at the trailing edge

$$\varDelta_s = \frac{2}{\pi} \int_0^\infty \frac{d}{d\xi_1} (\eta_1)_s \cdot \frac{(4a - \xi_1)}{(4a - \xi_1)^2 + (\eta_1')^2} d\xi_1 . \qquad \ldots \qquad \ldots \qquad \ldots \qquad (9)$$

Instead of evaluating this integral by the method of R. & M. 2107 we assume that, over a small interval $\xi_{1, n-1} < \xi_1, < \xi_{1,n}$, where $0 < \xi_1 < \infty$ is divided up into intervals not necessarily equal.

$$\frac{d(\eta_1)_s}{d\xi_1} = a_n = \text{const. for the } n\text{-th step.} \qquad \ldots \qquad \ldots \qquad \ldots \qquad \ldots \qquad (10)$$

Now

$$\int_{\xi_{1,n-1}}^{\xi_{1,n}} \frac{(4a - \xi_1) \, d\xi_1}{(4a - \xi_1)^2 + (\eta_1')^2} = \frac{1}{2} \log_e \frac{(4a - \xi_1, n - 1)^2 + (\eta_1')^2}{(4a - \xi_1, n)^2 + (\eta_1')^2} . \qquad \ldots \qquad \ldots \qquad \ldots \qquad \ldots \qquad (11)$$

Hence

$$\varDelta_s = \frac{2 \cdot 303}{\pi} \sum_{\eta=1}^{\infty} a_n \log_{10} \frac{(4a - \xi_1, n - 1)^2 + (\eta_1')^2}{(4a - \xi_1, n)^2 + (\eta_1')^2} . \qquad \ldots \qquad \ldots \qquad (12)$$

This is rapidly summed, as except near the trailing edge, comparatively large steps can be used and it is not necessary to go beyond $\xi_1 = 8a$. Also it will be found convenient to divide the logarithmic term by $4a$ in the numerator and the denominator.

If a quick answer is required, then we may take $4a \doteqdot c$ and $h_0 \doteqdot U_0$ and thus $(\eta_1)_s/4a$ becomes identical with δ_s^*/C to the degree of approximation except near the trailing edge.
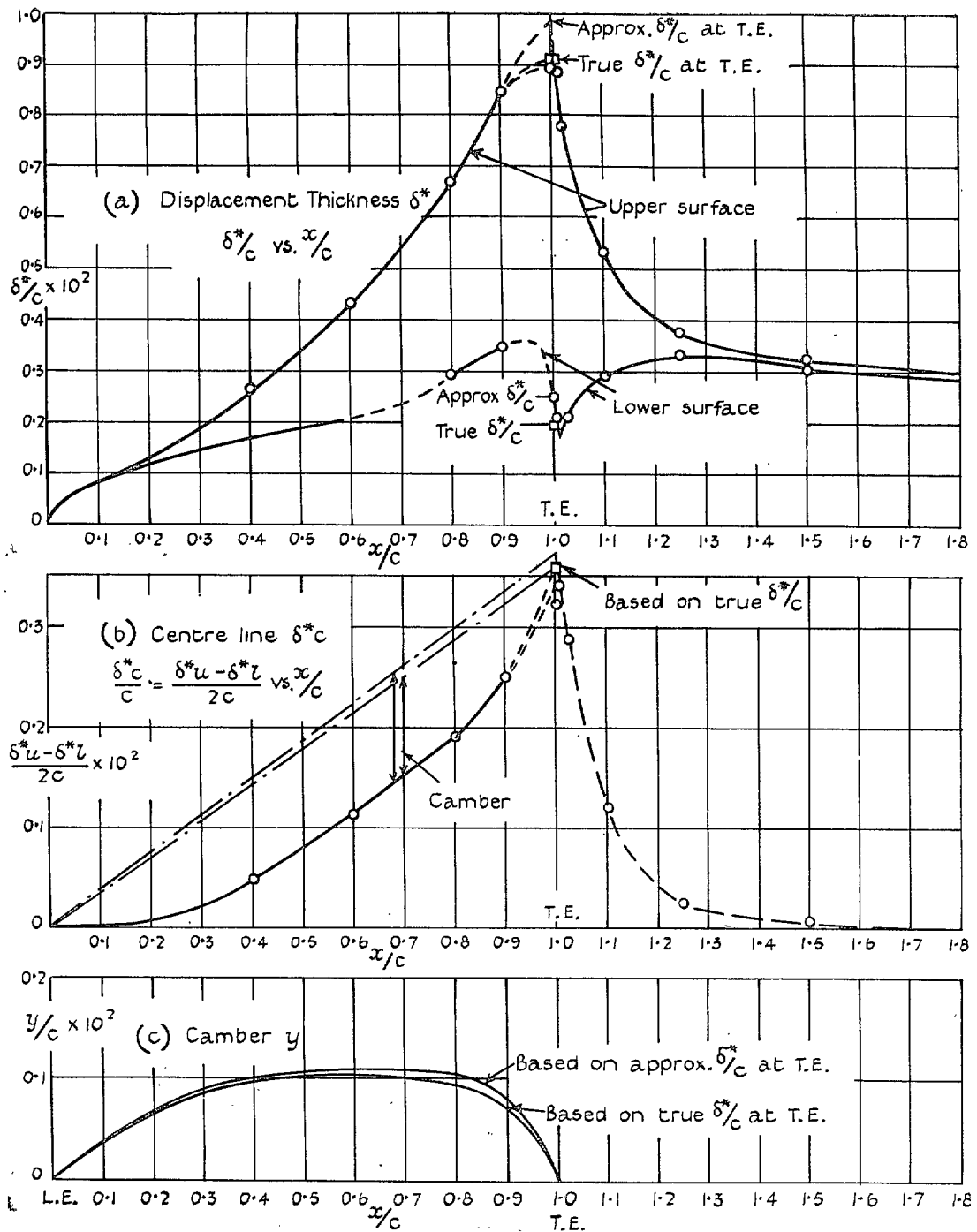
FIG. 9. Simple Joukowski aerofoil 11·8 per cent thick. Smooth. $\alpha = 6$ deg. $R = 4·2 \times 10^5$.
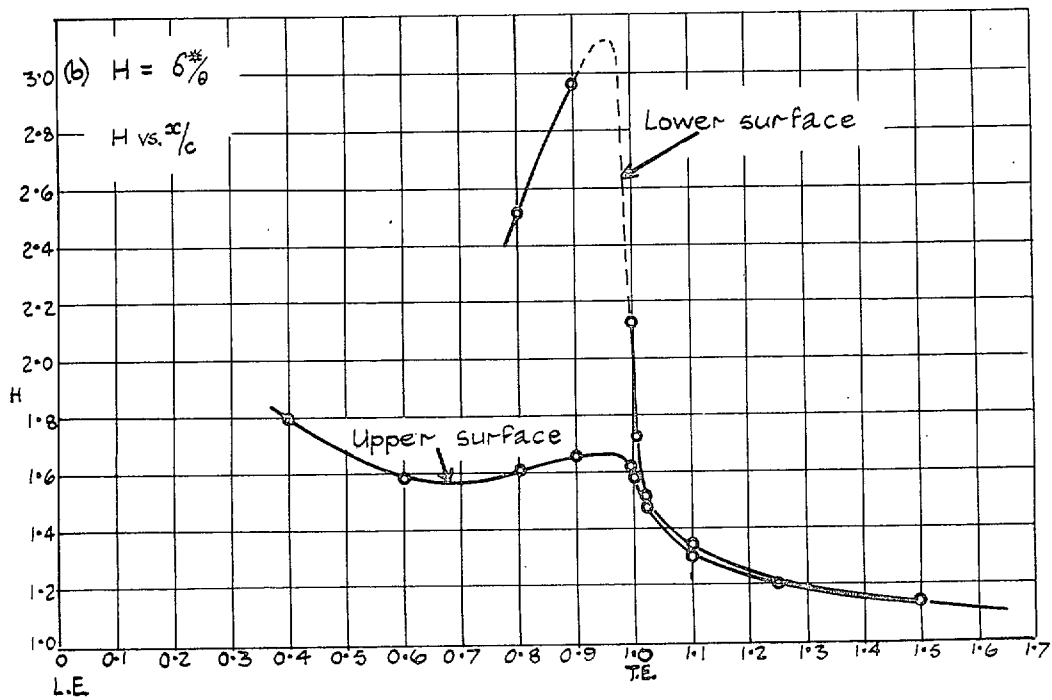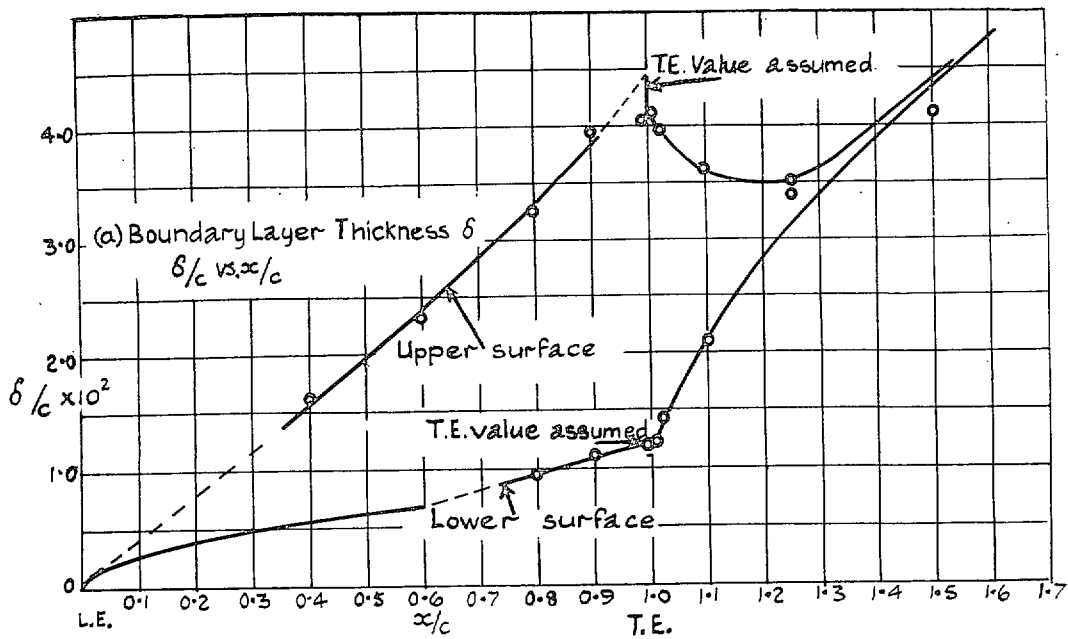
(a) Boundary Layer Thickness δ

δ/c vs. x/c

$\delta/c \times 10^2$

T.E. Value assumed

Upper surface

T.E. value assumed

Lower surface

L.E. x/c T.E.

(b) $H = \delta^*/\theta$

H vs. x/c

H

Lower surface

Upper surface

L.E.   T.E.

Fig. 10. Simple Joukowski aerofoil 11·8 per cent thick. Smooth. $\alpha = 6$ deg. $R = 4·2 \times 10^5$.

33

c

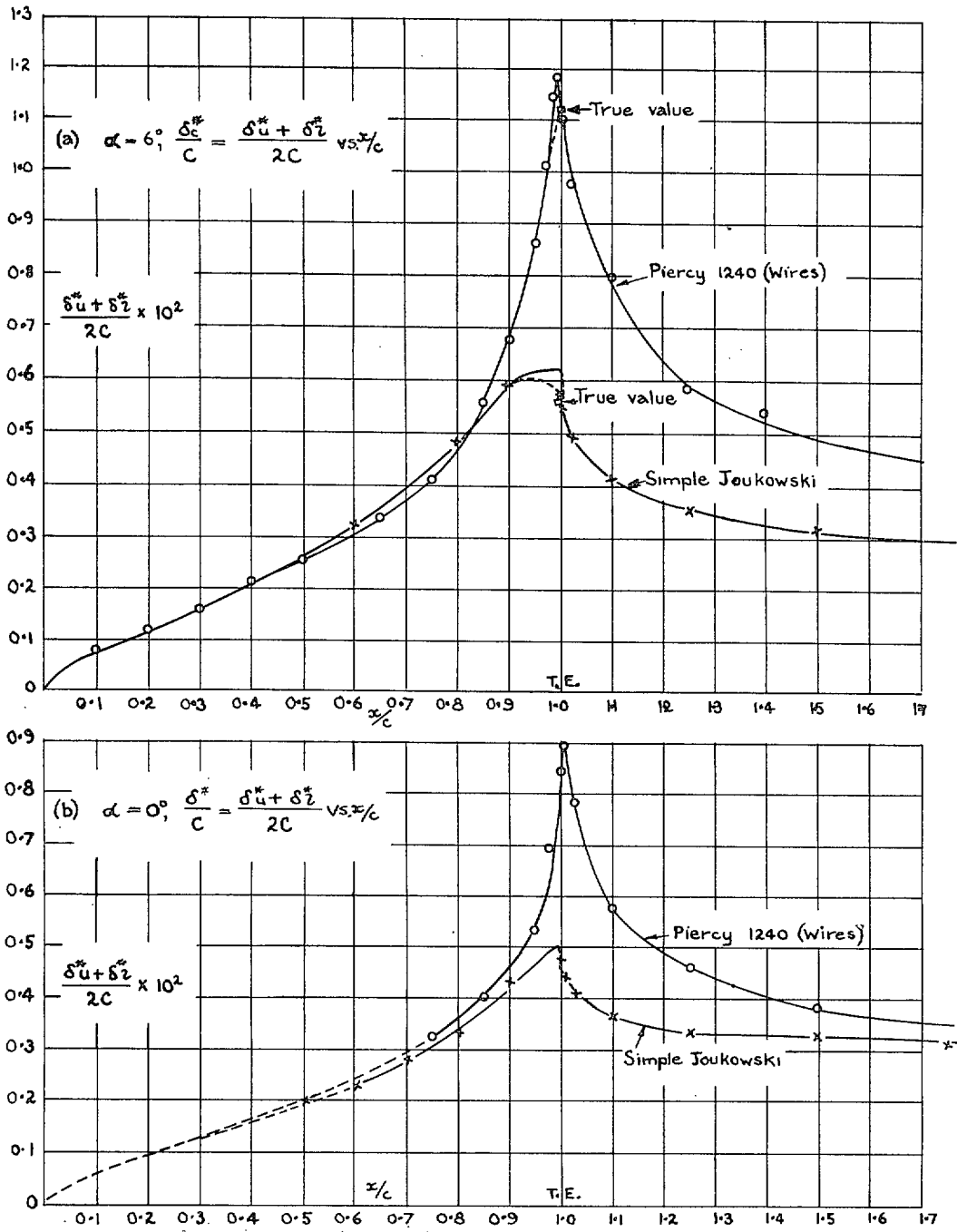FIG. 11.   Piercy 1240 aerofoil.   Turbulence wires. $\alpha = 6$ deg. $R = 4\cdot2 \times 10^5$.

34

Upper graph:

6·0

← T.E. value assumed

5·0

Upper surface

4·0 — Boundary layer thickness δ

δ/c vs. x/c

3·0

$\delta/c \times 10^{2}$

← T.E. value assumed

2·0

Lower surface

1·0

0

L.E. 0·1 0·2 0·3 0·4 0·5 0·6 0·7 0·8 0·9 1·0 T.E. 1·1 1·2 1·3 1·4 1·5 1·6 1·7

x/c

Lower graph:

2·6

(b) $H = \delta^*/\theta$

2·4

2·2 — H vs. x/c

2·0

Upper surface

H

1·8

1·6

Lower surface

1·4

1·2

1·0

0·1 0·2 0·3 0·4 0·5 0·6 0·7 0·8 0·9 1·0 T.E. 1·1 1·2 1·3 1·4 1·5 1·6 1·7

x/c
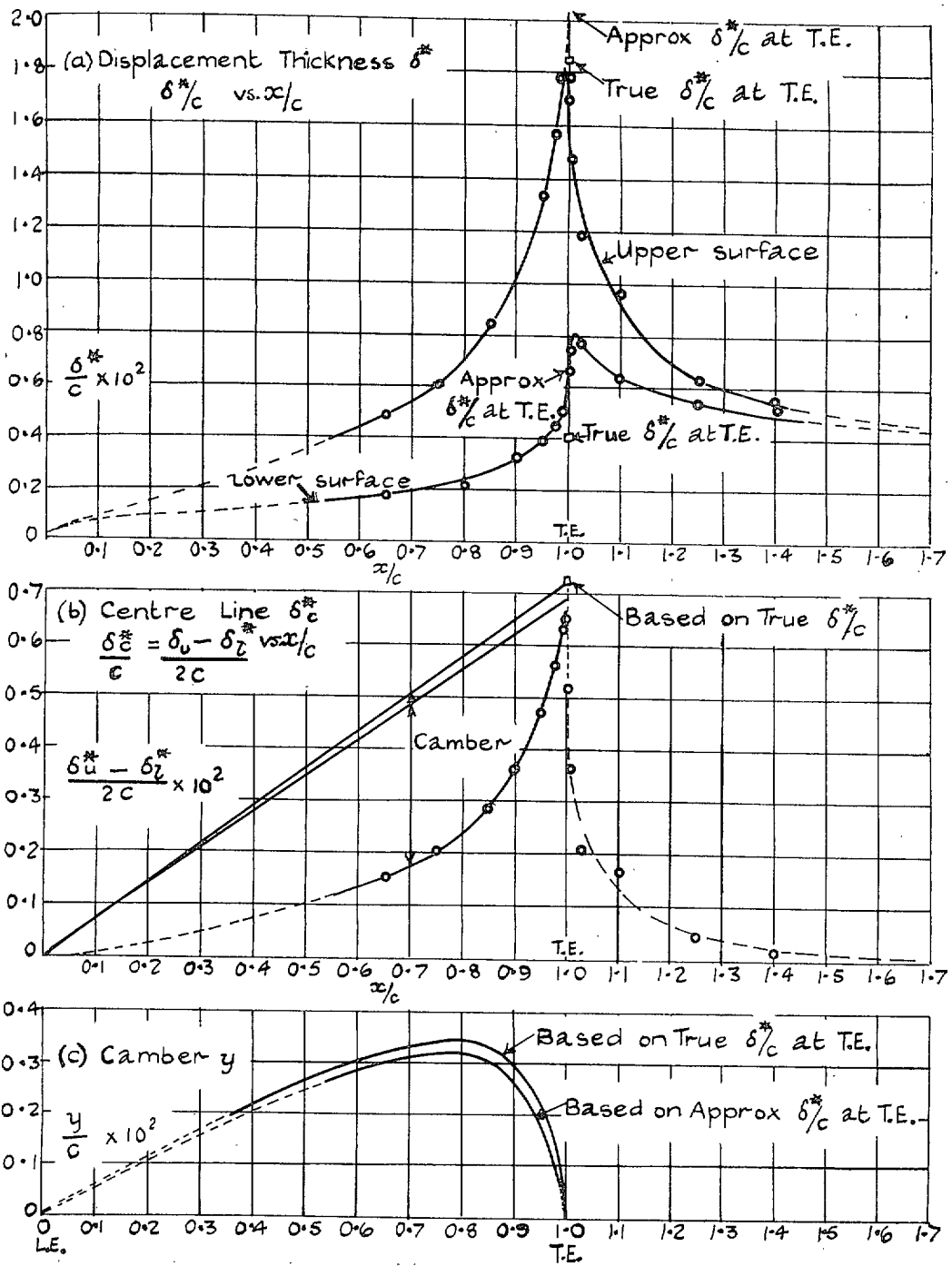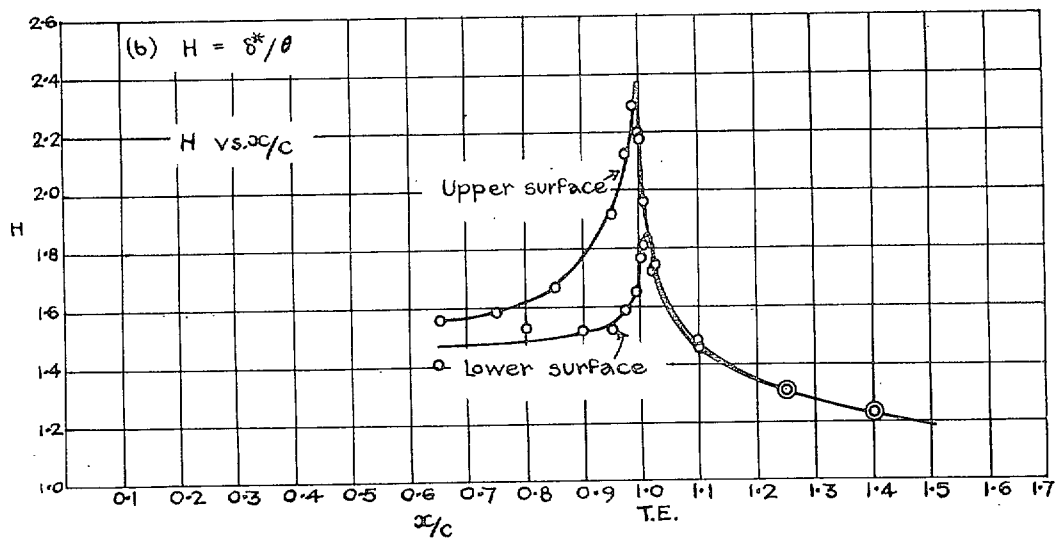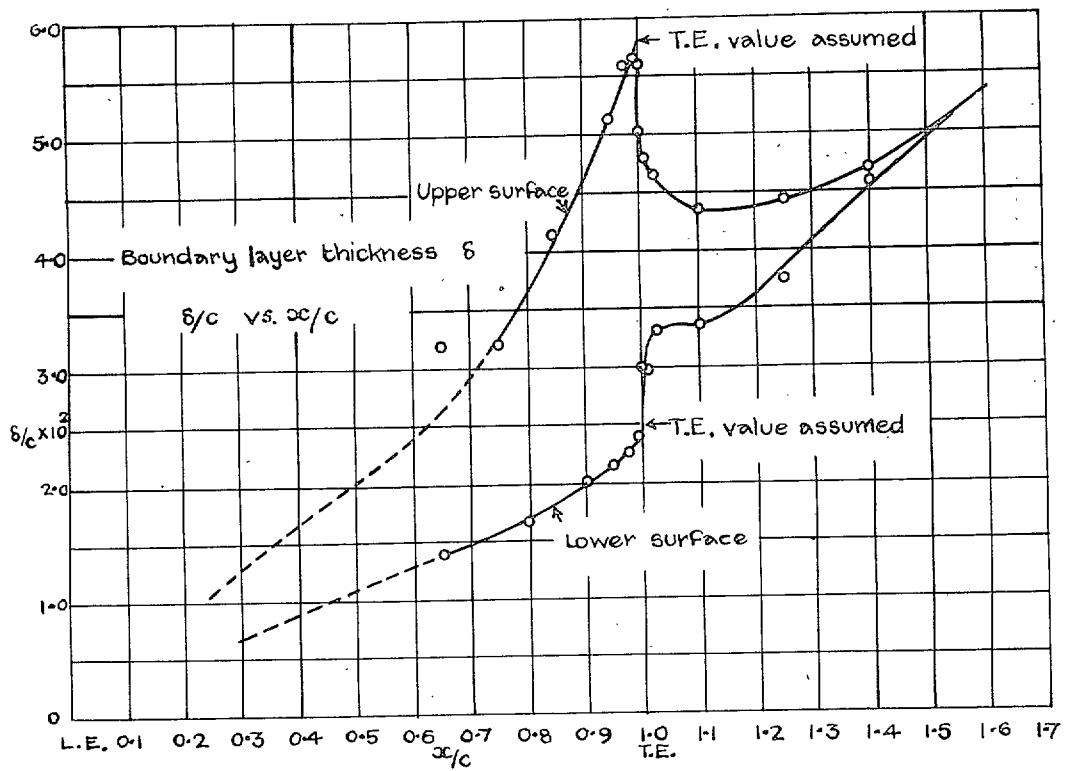
FIG. 12. Piercy 1240 aerofoil. Turbulence wires. $\alpha = 6$ deg. $R = 4 \cdot 2 \times 10^{5}$.

FIG.13. Mean displacement thickness δ_s^* for Joukowski and Piercy aerofoils. $R = 4 \cdot 2 \times 10^5$.
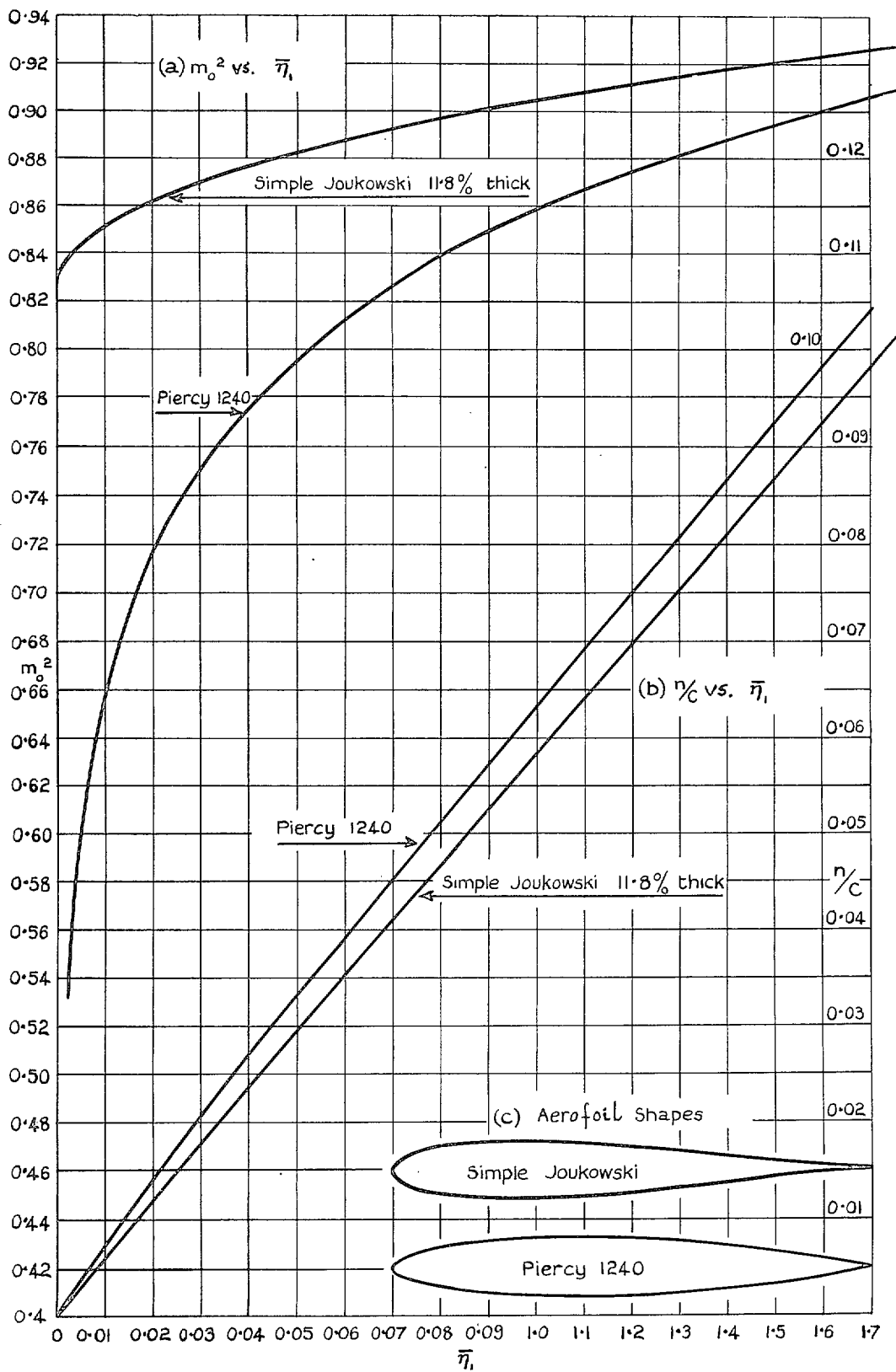
FIG. 14. $m_0{}^2$ and n/c against $\bar{\eta}_1$.
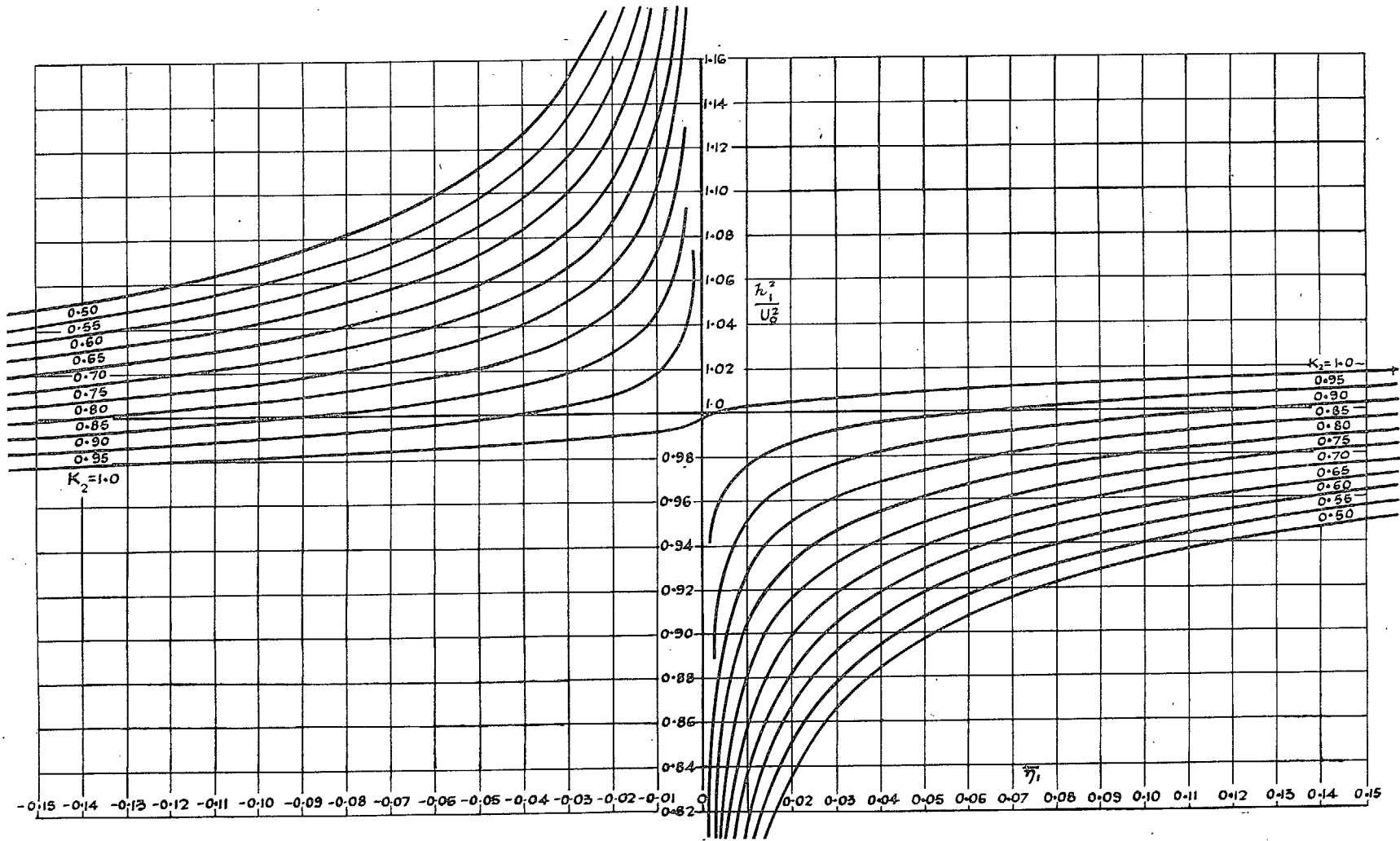
FIG. 15. (Velocity)^2 along a normal at trailing edge in plane of plate. $h_1{}^2/U_0{}^2$ against $\bar{\eta}_1$. $(\alpha - \alpha_1 - \alpha_2) = 3$ deg.
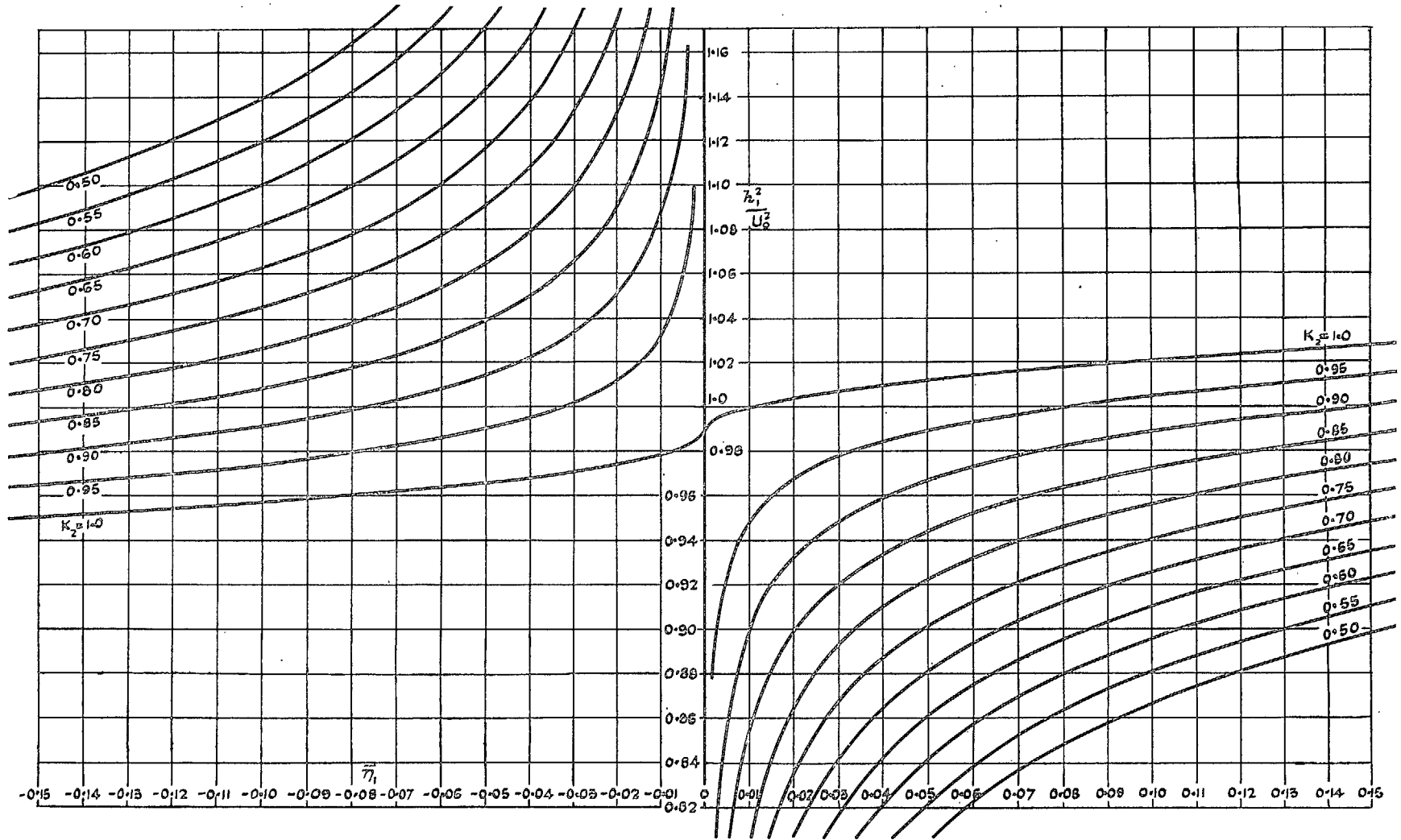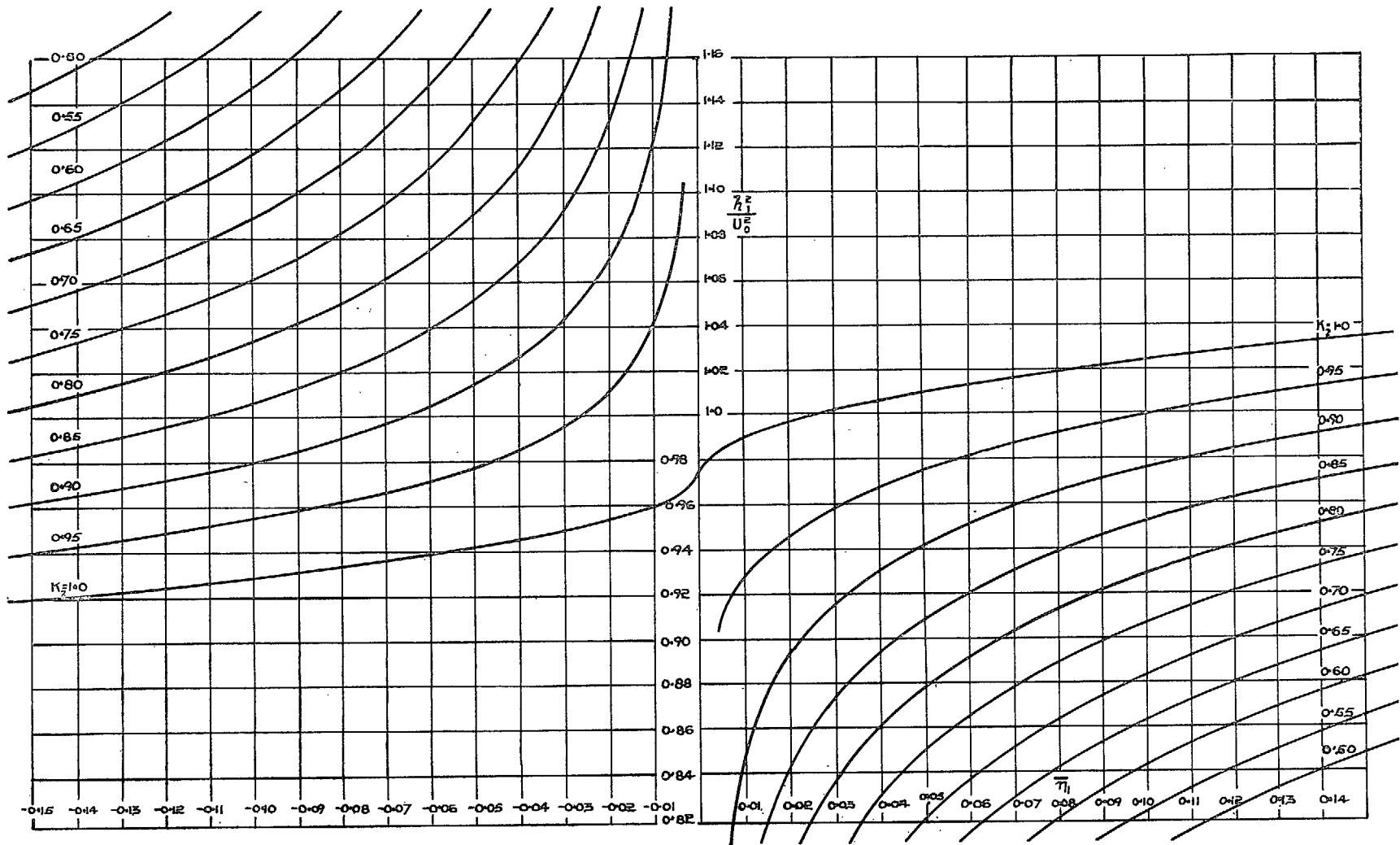
FIG. 16. (Velocity)^2 along a normal at trailing edge in plane of plate. $h_1{}^2/U_0{}^2$ against $\bar{\eta}_0$. $(\alpha - \alpha_1 - \alpha_2) = 6$ deg.

FIG. 17. (Velocity)^2 along a normal at trailing edge in plane of plate. $h_1{}^2/U_0{}^2$ against $\bar{\eta}_0$. $(\alpha - \alpha_1 - \alpha_2) = 9$ deg.

Publications of the
Aeronautical Research Council

ANNUAL TECHNICAL REPORTS OF THE AERONAUTICAL RESEARCH COUNCIL (BOUND VOLUMES)

1936 Vol. I. Aerodynamics General, Performance, Airscrews, Flutter and Spinning. 40*s.* (40*s.* 9*d.*)
    Vol. II. Stability and Control, Structures, Seaplanes, Engines, etc. 50*s.* (50*s.* 10*d.*)

1937 Vol. I. Aerodynamics General, Performance, Airscrews, Flutter and Spinning. 40*s.* (40*s.* 10*d.*)
    Vol. II. Stability and Control, Structures, Seaplanes, Engines, etc. 60*s.* (61*s.*)

1938 Vol. I. Aerodynamics General, Performance, Airscrews. 50*s.* (51*s.*)
    Vol. II. Stability and Control, Flutter, Structures, Seaplanes, Wind Tunnels, Materials. 30*s.* (30*s.* 9*d.*)

1939 Vol. I. Aerodynamics General, Performance, Airscrews, Engines. 50*s.* (50*s.* 11*d.*)
    Vol. II. Stability and Control, Flutter and Vibration, Instruments, Structures, Seaplanes, etc. 63*s.* (64*s.* 2*d.*)

1940 Aero and Hydrodynamics, Aerofoils, Airscrews, Engines, Flutter, Icing, Stability and Control, Structures, and a miscellaneous section. 50*s.* (51*s.*)

1941 Aero and Hydrodynamics, Aerofoils, Airscrews, Engines, Flutter, Stability and Control, Structures. 63*s.* (64*s.* 2*d.*)

1942 Vol. I. Aero and Hydrodynamics, Aerofoils, Airscrews, Engines. 75*s.* (76*s.* 3*d.*)
    Vol. II. Noise, Parachutes, Stability and Control, Structures, Vibration, Wind Tunnels 47*s.* 6*d.* (48*s.* 5*d.*)

1943 Vol. I. *(In the press.)*
    Vol. II. *(In the press.)*

ANNUAL REPORTS OF THE AERONAUTICAL RESEARCH COUNCIL—

1933–34	1*s.* 6*d.* (1*s.* 8*d.*)	1937	2*s.* (2*s.* 2*d.*)
1934–35	1*s.* 6*d.* (1*s.* 8*d.*)	1938	1*s.* 6*d.* (1*s.* 8*d.*)
April 1, 1935 to Dec. 31, 1936.	4*s.* (4*s.* 4*d.*)	1939–48	3*s.* (3*s.* 2*d.*)

INDEX TO ALL REPORTS AND MEMORANDA PUBLISHED IN THE ANNUAL TECHNICAL REPORTS, AND SEPARATELY—

April, 1950 - - - - R. & M. No. 2600. 2*s.* 6*d.* (2*s.* 7½*d.*)

AUTHOR INDEX TO ALL REPORTS AND MEMORANDA OF THE AERONAUTICAL RESEARCH COUNCIL—

1909–1949. R. & M. No. 2570. 15*s.* (15*s.* 3*d.*)

INDEXES TO THE TECHNICAL REPORTS OF THE AERONAUTICAL RESEARCH COUNCIL—

December 1, 1936 — June 30, 1939.	R. & M. No. 1850.	1*s.* 3*d.* (1*s.* 4½*d.*)
July 1, 1939 — June 30, 1945.	R. & M. No. 1950.	1*s.* (1*s.* 1½*d.*)
July 1, 1945 — June 30, 1946.	R. & M. No. 2050.	1*s.* (1*s.* 1½*d.*)
July 1, 1946 — December 31, 1946.	R. & M. No. 2150.	1*s.* 3*d.* (1*s.* 4½*d.*)
January 1, 1947 — June 30, 1947.	R. & M. No. 2250.	1*s.* 3*d.* (1*s.* 4½*d.*)
July, 1951.	R. & M. No. 2350.	1*s.* 9*d.* (1*s.* 10½*d.*)

Prices in brackets include postage.

Obtainable from

HER MAJESTY'S STATIONERY OFFICE